

Synthesis and Discovery of Pyrazine–Pyridine Biheteroaryl as a Novel Series of Potent Vascular Endothelial Growth Factor Receptor-2 Inhibitors

Gee-Hong Kuo,* Aihua Wang, Stuart Emanuel, Alan DeAngelis, Rui Zhang, Peter J. Connolly, William V. Murray, Robert H. Gruninger, Jan Sechler, Angel Fuentes-Pesquera, Dana Johnson, Steven A. Middleton, Linda Jolliffe, and Xin Chen

Drug Discovery Division, Johnson & Johnson Pharmaceutical Research and Development, L.L.C., 1000 Route 202, P.O. Box 300, Raritan, New Jersey 08869

Received May 6, 2004

Pathological angiogenesis is associated with disease states such as cancer, diabetic retinopathy, rheumatoid arthritis, endometriosis, and psoriasis. There is much evidence that direct inhibition of the kinase activity of vascular endothelial growth factor receptor-2 (VEGFR-2) will result in the reduction of angiogenesis and the suppression of tumor growth. Attempts to optimize a cyclin-dependent kinase-1 (CDK1) inhibitor by using palladium-catalyzed C–C bond, C–N bond formation reactions to assemble diverse biheteroaryl molecules led to the unexpected discovery of a pyrazine–pyridine biheteroaryl as a novel series of potent VEGFR-2 inhibitors. Compound **15**, which had $IC_{50} = 0.084 \mu M$ at VEGFR-2, showed very modest selectivity against fibroblast growth factor receptor-2 ($IC_{50} = 0.21 \mu M$), platelet-derived growth factor receptor ($IC_{50} = 0.36 \mu M$), and glycogen synthase kinase-3 ($IC_{50} = 0.478 \mu M$), while it exhibited more than 10-fold selectivity against epidermal growth factor receptor ($IC_{50} = 1.36 \mu M$) and insulin-R kinase ($IC_{50} = 1.69 \mu M$). On the other hand, compound **15** exhibited more than 100-fold selectivity against calmodulin kinase 2; casein kinase-1 and -2; CDK1 and -4; mitogen-activated protein kinase; and protein kinase A, $C\beta 2$, and $C\gamma$ ($IC_{50} > 10 \mu M$). Compound **15** also displayed high inhibitory potency on VEGF-stimulated human umbilical vein endothelial cell (HUVEC) proliferation ($IC_{50} = 0.005 \mu M$) and good selectivity against cell lines such as HUVEC, human aortic smooth muscle cells, and MRC5 lung fibroblasts. Molecular docking studies were conducted in an attempt to rationalize the unexpected high VEGFR-2 selectivity of **15**.

Introduction

Angiogenesis, the formation of new capillaries from preexisting blood vessels,¹ is a necessary process for organ development during embryogenesis and is critical for the female reproductive cycle, inflammation, and wound healing in the adult.² Pathological angiogenesis is associated with disease states such as cancer,³ diabetic retinopathy,⁴ rheumatoid arthritis,⁵ endometriosis,⁶ and psoriasis.⁷ Solid tumors, in particular, are dependent on angiogenesis to grow beyond a certain critical size by inducing new capillaries sprouting from existing blood vessels to secure their nutrition, oxygen supply, and waste removal.^{3,8} In addition, angiogenesis also promotes metastasis of tumor cells to other sites.⁹

The new vessel growth and maturation are highly complex and coordinated processes, requiring the stimulation by a number of growth factors,¹⁰ but vascular endothelial growth factor (VEGF) signaling often represents a critical rate-limiting step in physiological angiogenesis and pathological angiogenesis.¹¹ The biological effects of VEGF are mediated by two receptor tyrosine kinases (RTKs), VEGFR-1 (Flt-1)¹² and VEGFR-2 [also known as kinase domain region (KDR) or Flk-1].¹³ While the precise function of VEGFR-1 is still under debate,¹⁴ there is much evidence that VEGFR-2 is the major mediator of vascular endothelial cell (EC) mitogenesis and survival, as well as angiogenesis and

microvascular permeability.¹⁴ Therefore, it is expected that direct inhibition of the kinase activity of VEGFR-2 will result in the reduction of angiogenesis and the suppression of tumor growth. Furthermore, inhibition of VEGFR-2 targeting the genetically more stable host endothelial cells, instead of labile tumor tissues, may decrease the chance of resistance development.¹⁵

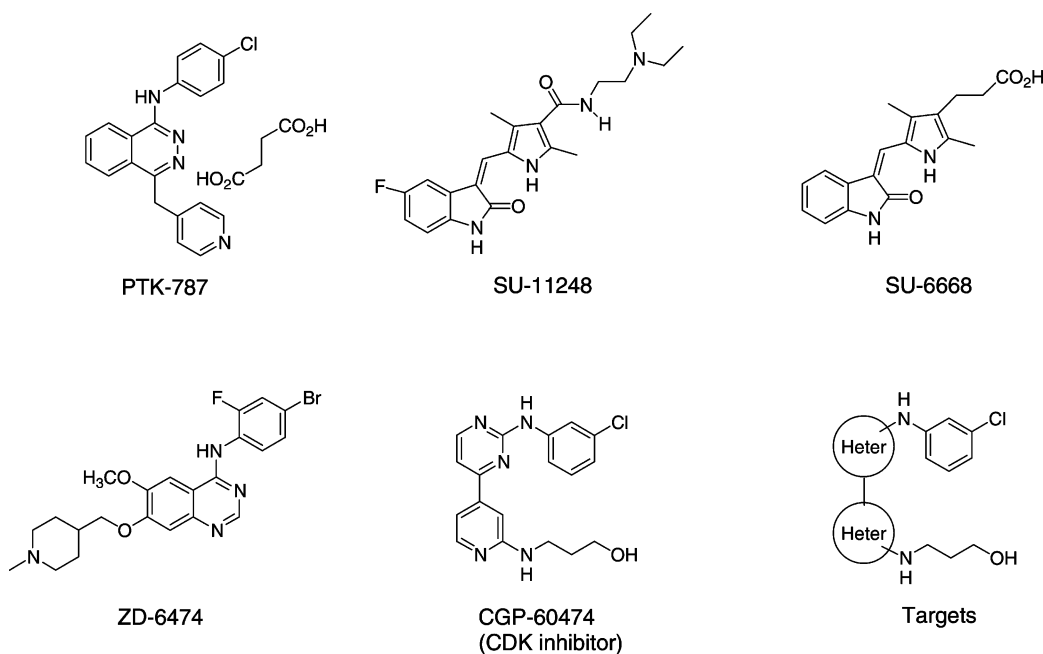
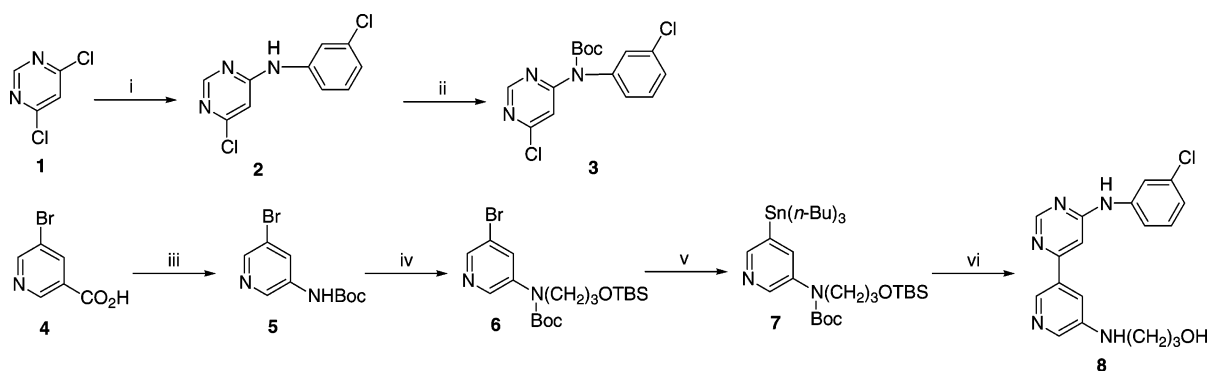
A number of VEGF inhibitors are currently undergoing advanced-stage clinical trials for the treatment of cancer, including a humanized monoclonal antibody to VEGF (bevacizumab/rhuMab VEGF),¹⁶ an anti-VEGFR-2 antibody,¹⁷ a soluble VEGF receptor,¹⁸ and several small molecule VEGFR-2 inhibitors (PTK787/vatalanib,¹⁹ SU-11248,²⁰ SU-6668,²¹ and ZD-6474,²² Scheme 1). Among them, bevacizumab (Avastin) in combination with chemotherapy,^{16,23} was accepted by the FDA in 2003 for the treatment of first-line metastatic colorectal cancer. This first proof-of-concept example will certainly warrant the development of many more small molecule VEGF inhibitors²⁴ for anti-angiogenesis therapy. This paper describes the unexpected discovery of the pyrazine–pyridine biheteroaryl scaffold as the basis of a novel series of potent VEGFR-2 inhibitors.

Chemistry

The chloride **3** was synthesized via a palladium-catalyzed C–N bond formation reaction²⁵ of 4,6-dichloropyrimidine **1** with 3-chloroaniline followed by Boc protection (Scheme 2). The required organostannane **7** was prepared in three-step sequence: (1) a Curtius

* To whom correspondence should be addressed. Tel: 908-704-4330. Fax: 908-203-8109. E-mail: gkuo@prdus.jnj.com.

Scheme 1

Scheme 2^a

^a (i) 3-chloroaniline, Pd(OAc)₂, BINAP, NaOt-Bu, 90 °C; (ii) Boc₂O, DMAP; (iii) DPPA, Et₃N, *t*-BuOH, 65–95 °C; (iv) Br(CH₂)₃OTBS, Cs₂CO₃, 70 °C; (v) [(*n*-Bu)₃Sn]₂, Pd(OAc)₂, P(*o*-Tol)₃, 100 °C; (vi) (a) **3**, Pd₂(dba)₃, AsPh₃, 67 °C, (b) TFA.

rearrangement²⁶ of the nicotinic acid **4** with DPPA gave **5**, (2) alkylation of **5** with the silyl-protected bromide gave **6**, (3) a palladium-catalyzed transformation of the organo halide to the organostannane²⁷ provided **7**. The first biheteroaryl target, pyrimidine–pyridine **8**, was synthesized by a palladium-catalyzed Stille coupling reaction²⁸ of halide **3** with organostannane **7** followed by deprotection with TFA (Scheme 2).

The second target, pyrazine–pyridine **15**, was prepared by a different reaction sequence (Scheme 3). The Stille coupling reaction of organostannane **10** with 2,6-dichloropyrazine catalyzed by Pd(PPh₃)₂Cl₂²⁹ gave **11**. Palladium-catalyzed C–N bond formation of **11** with 3-chloroaniline in the presence of DPPF³⁰ as the ligand generated **12** in good yield. Boc-protection and base hydrolysis, followed by Curtius rearrangement, provided **14**. Alkylation of **14** with the silyl-protected bromide, followed by TFA deprotection, gave the second target molecule **15**. The biheteroaryl targets of **20**, **25**, and **30** were all prepared in a similar way as **15** (Scheme 3).

The synthesis of pyrazine–pyridine **38** was shown in Scheme 4. Under the same reaction conditions used in the preparation of chloride **2** (Pd(OAc)₂, BINAP, NaOt-Bu), chloride **32** was formed in 90% yield instead of 4%

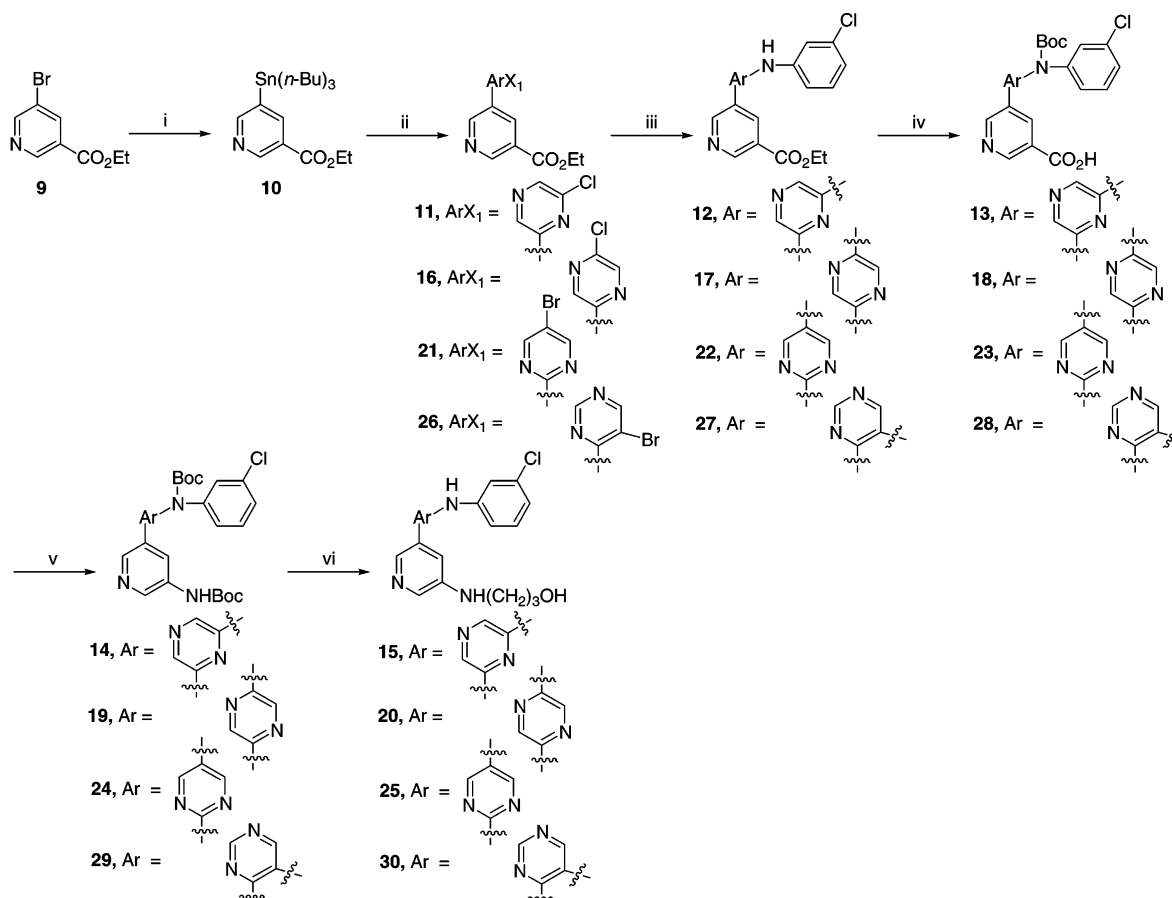
yield as in chloride **2**. The known **34**³¹ was converted to the organostannane **35**, followed by the Stille coupling reaction with **33** to afford **36**. Base hydrolysis, Curtius rearrangement, alkylation, and deprotection provided the target molecule **38**.

The synthesis of pyrazine–pyridine **42** was shown in Scheme 5. Starting from the bromide **39**, Boc protection, alkylation and palladium-catalyzed transformation gave the organostannane **41**. Stille coupling reaction of **41** with **33**, followed by deprotection afforded target **42**.

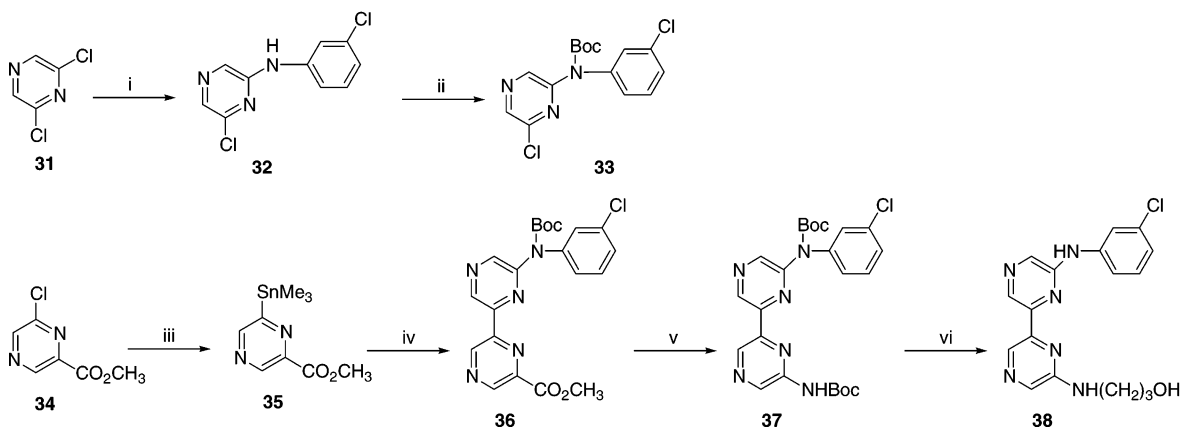
The synthesis of biheteroaryl **47** was shown in Scheme 6. A Curtius rearrangement was conducted on **43**³² to give **44**. Alkylation, organostannane formation, and Stille coupling reaction, followed by deprotection, gave the target **47**.

To our delight, the nucleophilic organostannane **48**³³ survived the Curtius rearrangement reaction condition to generate the *N*-Boc-substituted (trimethylstannanyl)-pyridine **49** in 57% yield (Scheme 7). A Stille coupling reaction of **49** with **33**, followed by alkylation and deprotection, generated the pyrazine–pyridine **51**.

Transformation of the known triflate **52**³⁴ to the corresponding organostannane, followed by the Stille coupling reaction, gave **53** (Scheme 8). Base hydrolysis,

Scheme 3^a

^a (i) [(*n*-Bu)₃Sn]₂, Pd(OAc)₂, P(*o*-Tol)₃, 100 °C; (ii) ArX₁X₂, Pd(PPh₃)₂Cl₂, LiCl, 100 °C; (iii) 3-chloroaniline, Pd₂(dba)₃, DPPF, Cs₂CO₃, 110 °C; (iv) (a) Boc₂O, DMAP, (b) NaOH, 0–20 °C; (v) DPPA, Et₃N, *t*-BuOH, 65–100 °C; (vi) (a) Br(CH₂)₃OTBS, Cs₂CO₃, 70 °C, (b) TFA.

Scheme 4^a

^a (i) 3-chloroaniline, Pd(OAc)₂, BINAP, NaO*t*-Bu, 80 °C; (ii) Boc₂O, DMAP; (iii) Pd(PPh₃)₄, Me₆Sn₂, LiCl, BHT, 100 °C; (iv) **33**, Pd(PPh₃)₂Cl₂, LiCl, 100 °C; (v) (a) LiOH, (b) DPPA, Et₃N, *t*-BuOH, 60–95 °C; (vi) (a) Br(CH₂)₃OTBS, Cs₂CO₃, 70 °C, (b) TFA.

followed by the Curtius rearrangement, alkylation, and deprotection, afforded the target molecule **55**.

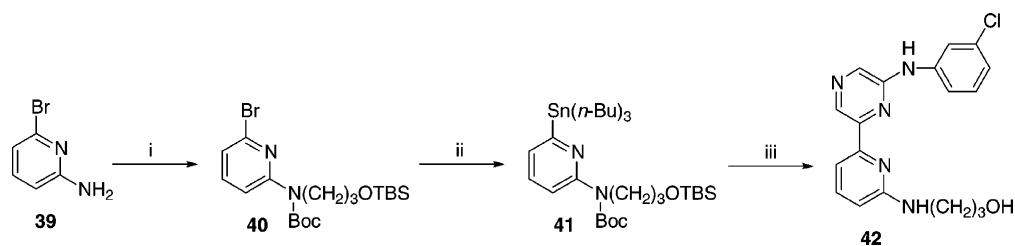
The synthesis of the pyrazine–thiazole **59** was started from the aminothiazole **56** (Scheme 9). Boc-protection and alkylation gave **58**, which was converted to the corresponding organostannane, followed by the Stille coupling reaction and deprotection, generating the target **59**.

The target, pyrazine–oxazole **62**, was synthesized via a different method (Scheme 10). A hetero-Heck reaction³⁵ of **33** with oxazole in the presence of Pd(PPh₃)₄

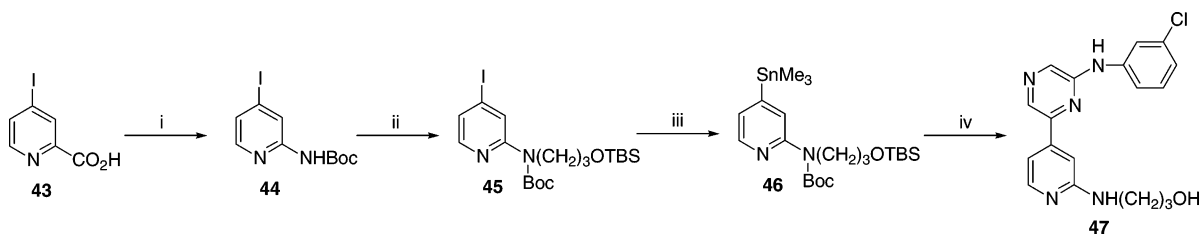
gave **60** directly. Iodination³⁶ followed by the amination gave the target **62**.

Results and Discussion

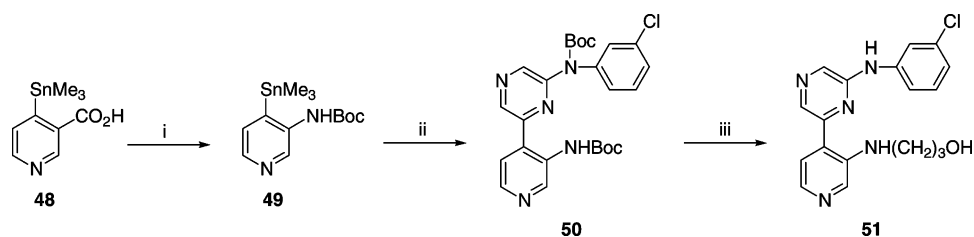
Lead Discovery. We were originally interested in identifying potent and selective cyclin-dependent kinase-1 (CDK1) inhibitors for the treatment of cancer.³⁷ In a literature review, discovery and lead optimization efforts have provided many CDK inhibitors over the past decade;³⁸ two of these agents, flavopiridol and UCN-01,

Scheme 5^a

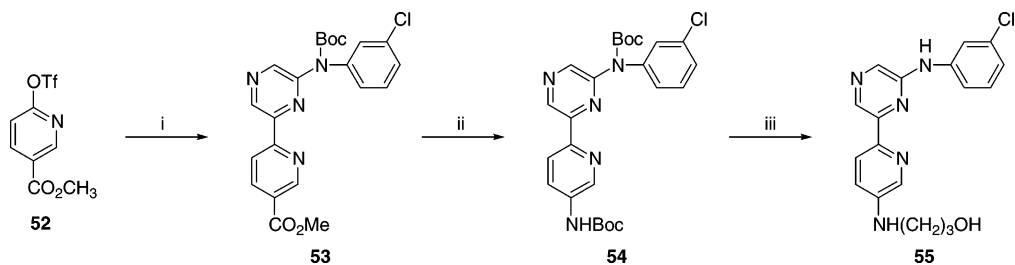
^a (i) (a) Boc_2O , DMAP, (b) $\text{Br}(\text{CH}_2)_3\text{OTBS}$, Cs_2CO_3 , 70 °C; (ii) $\text{Pd}(\text{PPh}_3)_4$, $[(n\text{-Bu})_3\text{Sn}]_2$, LiCl, BHT, 100 °C; (iii) (a) **33**, $\text{Pd}(\text{PPh}_3)_2\text{Cl}_2$, LiCl, 100 °C, (b) TFA.

Scheme 6^a

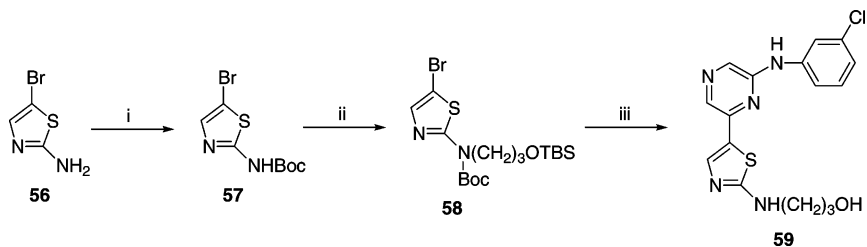
^a (i) DPPA, Et_3N , *t*-BuOH, 65–95 °C; (ii) $\text{Br}(\text{CH}_2)_3\text{OTBS}$, Cs_2CO_3 , 70 °C; (iii) Me_6Sn_2 , $\text{Pd}(\text{PPh}_3)_4$, LiCl, BHT, 90 °C; (iv) (a) **33**, $\text{Pd}(\text{PPh}_3)_2\text{Cl}_2$, LiCl, 100 °C, (b) TFA.

Scheme 7^a

^a (i) DPPA, Et_3N , *t*-BuOH, 65–95 °C; (ii) **33**, $\text{Pd}(\text{PPh}_3)_2\text{Cl}_2$, LiCl, 100 °C; (iii) (a) $\text{Br}(\text{CH}_2)_3\text{OTBS}$, Cs_2CO_3 , 70 °C, (b) TFA.

Scheme 8^a

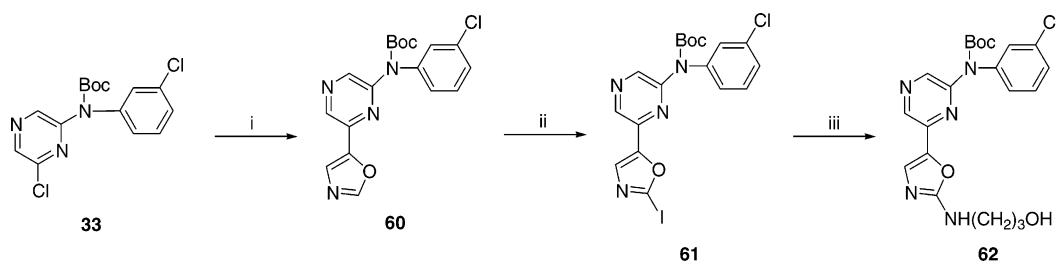
^a (i) (a) $\text{Pd}(\text{PPh}_3)_4$, Me_6Sn_2 , LiCl, BHT, 100 °C, (b) **33**, $\text{Pd}(\text{PPh}_3)_2\text{Cl}_2$, LiCl, 100 °C; (ii) (a) LiOH, (b) DPPA, Et_3N , *t*-BuOH, 65–95 °C; (iii) (a) $\text{Br}(\text{CH}_2)_3\text{OTBS}$, Cs_2CO_3 , 70 °C, (b) TFA.

Scheme 9^a

^a (i) Boc_2O , DMAP; (ii) $\text{Br}(\text{CH}_2)_3\text{OTBS}$, Cs_2CO_3 , 70 °C; (iii) (a) $\text{Pd}(\text{PPh}_3)_4$, $[(n\text{-Bu})_3\text{Sn}]_2$, LiCl, BHT, 100 °C, (b) **33**, $\text{Pd}(\text{PPh}_3)_2\text{Cl}_2$, LiCl, 100 °C; (c) TFA.

have advanced to clinical evaluation.^{39,40} However, both flavopiridol⁴¹ and UCN-01⁴² proved to be potent but nonselective CDK inhibitors. Recently, a high-affinity CDK1 inhibitor (CGP-60474, $\text{IC}_{50} = 0.017 \mu\text{M}$, Scheme 1) with better selectivity toward other kinases was

reported.⁴³ Therefore, we decided to take advantage of the recent advances in palladium-catalyzed C–C bond, C–N bond formation reactions to assemble diverse biheteroaryl molecules (Scheme 1), which might be difficult to synthesize otherwise, with the goal to

Scheme 10^a

^a (i) oxazole, Pd(PPh₃)₄, AcOK, 80 °C; (ii) LHMDS, -78 °C, diiodoethane; (iii) 3-amino-1-propanol, 100 °C.

Table 1. Binding Affinities at CDK1 and VEGFR-2^a

Compd	Heteroaryl	IC ₅₀ ± SEM ^b (μM)	
		CDK1	VEGFR-2
8		2.40 ± 0.56	>10
15		>10	0.084 ± 0.014
20		>10	>10
25		>10	>10
30		>10	>10

^a Assay details are described in the Experimental Section.

^b SEM: standard error of the mean.

identify a CDK1 inhibitor with optimized potency, selectivity, and pharmacokinetic profiles.

We first prepared pyrimidine–pyridine **8** (Table 1), a close analogue of CGP-60474, by moving the bottom nitrogen atom in the pyridine ring to the meta-position and moving one of the pyrimidine nitrogen atoms from the ortho- to the para-position relative to the (3-chlorophenyl)amino group. A 140-fold decrease in CDK1 inhibitory potency (**8**, IC₅₀ = 2.4 μM, Table 1) was observed together with very poor inhibition against VEGFR-2 (IC₅₀ > 10 μM), one of the kinases in our selectivity panel.

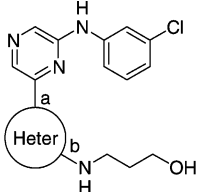
We then replaced the upper pyrimidine ring with a pyrazine ring while the lower pyridine ring remained unchanged to give **15**. To our surprise, the inhibition at CDK1 was totally abolished (**15**, IC₅₀ > 10 μM) while a high potency was observed at VEGFR-2 (**15**, IC₅₀ = 0.084 μM). The nitrogen atoms in the upper ring of these biheteroaryls clearly play a major role in the binding affinities of the inhibitors for CDK1 and VEGFR-2.

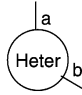
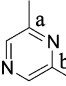
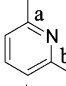
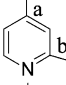
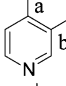
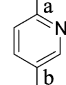
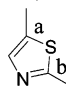
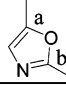
Shifting the (3-chlorophenyl)amino group from the meta- to the para-position in the upper pyrazine ring abolished the kinase inhibition of both CDK1 and VEGFR-2 (**20**, IC₅₀ > 10 μM, IC₅₀ > 10 μM). Apparently, the relative position of the substituted aniline moiety to the upper ring is also critical to the binding affinities at the kinases. The poor kinase inhibitory potency of **25** and **30** (IC₅₀ > 10 μM at both CDK1 and VEGFR-2) further suggested the importance of the 1,3-orientation between the substituted-aniline group and the lower ring moiety to the kinase activities.

With the discovery of the potent (IC₅₀ = 0.084 μM) and selective (>100-fold against CDK1) VEGFR-2 inhibitor **15** in hand, we continued to explore the impact of the lower ring of the biheteroaryl toward the VEGFR-2 inhibition. Replacing the pyridine of **15** with another pyrazine gave **38**. The addition of one extra nitrogen atom to the lower ring reduced by 6-fold the potency at VEGFR-2 (**38**, IC₅₀ = 0.497 μM, Table 2). Removal of one nitrogen atom from the lower meta-position of **38** did not restore the potency (**42**, IC₅₀ > 10 μM for both kinases). By comparing compounds **15** (IC₅₀ = 0.084 μM), **38** (IC₅₀ = 0.497 μM), and **42** (IC₅₀ > 10 μM), the significant contribution of the nitrogen atom at the meta-position of the lower ring to the VEGFR-2 inhibition was demonstrated; on the other hand, the nitrogen atom at the ortho-position between the two substituents on the lower ring was detrimental to the binding affinity at VEGFR-2.

Replacing the 3-pyridine of **15** with 4-pyridine (as in CGP-60474) gave **47**. Interestingly, compound **47** displayed significant inhibition at both VEGFR-2 and CDK1 (**47**, IC₅₀ = 0.5 μM at both kinases). Shifting the (hydroxypropyl)amino side chain of **47** from the meta-position to the ortho-position resulted in **51** with reduced potency at both kinases (**51**, IC₅₀ = 0.761 μM at VEGFR-2; IC₅₀ = 2.22 μM at CDK1). By comparison of CGP-60474 (IC₅₀ = 0.017 μM at CDK1) and **47** (IC₅₀ = 0.5 μM at CDK1) to **15** (IC₅₀ > 10 μM at CDK1), the nitrogen atom at the para-position of the lower ring (4-pyridine) (such as in CGP-60474 and **47**) appears to contribute to the binding affinity at CDK1 more significantly than at VEGFR-2.

If we shifted the (hydroxypropyl)amino side chain of **42** from the meta-position to the para-position to generate **55**, no inhibition was observed at either kinases (**55**, IC₅₀ > 10 μM for VEGFR-2 and CDK1). We next replaced the lower 3-pyridine of **15** with a thiazole to give **59**, and about 8-fold reduced potency at VEGFR-2 was observed for **59** when compared to **15** (**59**, IC₅₀ = 0.708 μM at VEGFR-2). Replacement of the 3-pyridine of **15** with an oxazole afforded **62** with even lower potency at VEGFR-2 (**62**, IC₅₀ = 2.11 μM). These

Table 2. Binding Affinities at CDK1 and VEGFR-2^a


Compd		IC ₅₀ ± SEM (μM)	
		CDK1	VEGFR-2
38		>10	0.497 ± 0.125
42		>10	>10
47		0.500 ± 0.120	0.500 ± 0.145
51		2.22 ± 0.49	0.761 ± 0.189
55		>10	>10
59		8.08 ± 1.93	0.708 ± 0.292
62		>10	2.11 ± 0.54

^a Assay details are described in the Experimental Section.

observations were consistent with the notion that “the thiazole is a closer bioisosteres⁴⁴ of pyridine than oxazole”.

In summary, while no improvement was made toward the potency and selectivity at CDK1 with the diverse biheteroaryls examined, we unexpectedly discovered that compound **15**, having a pyrazine–pyridine scaffold with 1,3-substitution-orientation at both upper and lower rings, exhibited high potency at VEGFR-2 and high selectivity against CDK1.

Kinase Selectivity. We next examined the selectivity of the most potent VEGFR-2 inhibitor, **15** (IC₅₀ = 0.084 μM), against a representative panel of kinases (Table 3). Compound **15** showed very modest selectivity (2–5-fold) against fibroblast growth factor receptor (FGFR-2, IC₅₀ = 0.21 μM), platelet-derived growth factor receptor (PDGF-R, IC₅₀ = 0.36 μM), and glycogen synthase kinase-3 (GSK-3, IC₅₀ = 0.478 μM), while it exhibited more than 1 order of magnitude of selectivity against epidermal growth factor receptor (EGFR, IC₅₀ = 1.36 μM) and insulin-R kinase (IC₅₀ = 1.69 μM). FGFR-2 and PDGF-R have been implicated indirectly in inducing VEGF secretion and hence in angiogenesis.⁴⁵ ST1-571 (Gleevec) is a potent PDGF-R inhibitor and a v-Abl inhibitor. It has been approved recently for the treatment of chronic myeloid leukemia and KIT positive metastatic malignant gastrointestinal stromal tumors

Table 3. IC₅₀ (μM) for Selected Kinase Assays for **15**^a

kinase assay	IC ₅₀	kinase assay	IC ₅₀
VEGFR-2	0.084	GSK-3	0.478
calmodulin kinase-2	>10	insulin-R kinase	1.69
casein kinase-1	>10	MAPK (ERK2)	>10
casein kinase-2	>10	PDGF-R	0.36
CDK1	>10	PKA	>10
CDK4	>10	PKCβ2	>10
EGFR	1.36	PKCγ	>10
FGFR-2	0.21		

^a Assay details are described in the Experimental Section. IC₅₀ values are reported as the average of at least two separate determinations.

Table 4. IC₅₀ (μM) for Inhibition of Cell Proliferation by **15**^a

cell line	IC ₅₀ ± SEM	cell line	IC ₅₀ ± SEM
VEGF-stimulated HUVEC	0.005 ± 0.003	HeLa	>10
HUVEC	1.68 ± 0.146	HCT-116	>10
HASMC	3.87 ± 0.168	A375	>10
MRC5	6.6 ± 0.110		

^a Assay details are described in the Experimental Section.

and is under investigation in the treatment of glioblastomas which exploits its PDGFR inhibitory activity.⁴⁶ Therefore, although we were targeting the VEGFR inhibition, the very modest selectivity of compound **15** against FGFR-2 and PDGF-R may not be undesirable. On the other hand, compound **15** exhibited at least 2 orders of magnitude of selectivity against calmodulin kinase 2, casein kinase-1 or -2, CDK1, CDK4, mitogen-activated protein kinase (MAPK), protein kinase A (PKA), protein kinase Cβ2 (PKCβ2), and protein kinase Cγ (PKCγ) (IC₅₀ >10 μM, Table 3).

Cellular Selectivity. The cellular activity of the compound was tested for its ability to inhibit VEGF-stimulated proliferation of human umbilical vein endothelial cells (HUVEC). Compound **15** exhibits excellent cellular potency (IC₅₀ = 0.005 μM, Table 4) for inhibiting VEGF-stimulated proliferation.⁴⁷ On the other hand, compound **15** only displayed modest effect on the unstimulated growth of HUVEC (IC₅₀ = 1.68 μM). The 336-fold difference in potency of compound **15** for inhibition of VEGF-stimulated growth of HUVEC versus unstimulated growth of HUVEC may suggest its specificity of action through inhibition of VEGFR signal transduction. In addition, compound **15** displayed very minimal inhibition of proliferation of two normal human cell types, human aortic smooth muscle cells (HASMC, IC₅₀ = 3.87 μM) and MRC5 lung fibroblasts (IC₅₀ = 6.6 μM), which indicates the high cellular selectivity of compound **15** for VEGF-mediated processes.

The ability of compound **15** to inhibit the proliferation of cells derived from carcinomas originating from various tissues such as HeLa (cervical adenocarcinoma), HCT-116 (colon carcinoma), and A375 (malignant melanoma) was also examined. The lack of inhibition of the growth of these tumor cell lines (IC₅₀ >10 μM, Table 4) further confirms that the VEGFR inhibitor **15** does not exhibit general antiproliferative activity, as would occur through inhibition of growth regulatory kinases such as CDK1 inhibitors.

Molecular Docking Studies. In an attempt to rationalize the unexpected high kinase selectivity of pyrazine–pyridine biheteroaryl **15** at VEGFR-2 over CDK1, molecular docking studies of CGP-60474 and **15**

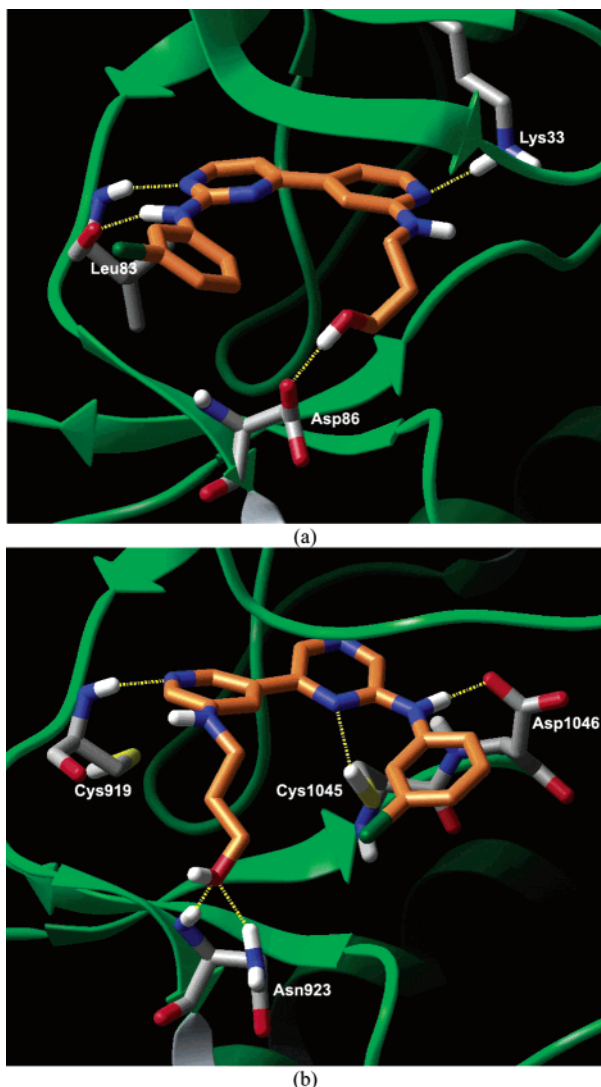


Figure 1. Illustration of the binding modes of CGP60474 (a) and **15** (b) in the ATP-binding sites of CDK1 and VEGFR-2, respectively, suggested by molecular docking. The ligands and the key residues that act as their hydrogen-bonding partners are represented in the tube model, while the proteins are in the cartoon model. The hydrogen bonds are indicated by the yellow dotted lines. (Atom color scheme: hydrogen in white, oxygen in red, nitrogen in blue, chlorine in dark green, carbon on ligands in orange, and carbon on proteins in gray.)

on CDK1 and VEGFR-2 were conducted, respectively. Their favorite docking poses in the ATP-binding sites are illustrated in Figure 1. Overall, both compounds show a nice fit in the binding sites and make extensive favorable van der Waals contacts with proteins through their tricyclic scaffolds. Interestingly, they adopt two opposite binding modes, in terms of hydrogen bonding. CGP-60474 (Figure 1a) adopts a typical bidentate hydrogen-bonding mode with the CDK1 backbone at the hinge region, as described by Furet et al.,⁴⁸ the pyrimidine nitrogen with the amide nitrogen of Leu83, and the anilino nitrogen with the carbonyl oxygen of Leu83. Two additional hydrogen bonds may also be formed, one is between the pyridine nitrogen and the terminal amino group of Lys33, and the other one is between the hydroxyl group and the terminal carboxylate group of Asp86. On the other hand, compound **15** (Figure 1b) adopts a single hydrogen bond to interact with the

VEGFR-2 backbone at the hinge region, i.e., the pyridine nitrogen and the amide nitrogen of Cys919. Meanwhile, the anilino nitrogen is moving away from the hinge region and is hydrogen bonded to the carboxylate group of Asp1046. Three additional hydrogen bonds may also be formed, one is between the inner pyrazine nitrogen with the thiol group of Cys1045, and the other two are between the hydroxyl group of **15** and the residue Asn923. The hydrogen bond between the inner pyrazine nitrogen and the thiol group of Cys1045 may be pivotal, because it allows the pyrazine ring to get close to the bulky thiol group of Cys1045, and therefore, **15** may simultaneously form the above two hydrogen bonds with Cys919 and Asp1046.

The results of molecular docking studies may provide us some insights into the SAR observed in Tables 1 and 2 as well. First, the 1,3-disubstitution pattern at both of the upper and lower rings appears critical, since the tricyclic scaffold needs to adopt a U-shape conformation to fit into the ATP-binding site. Any different disubstitution patterns may change the overall shape of the scaffold and reduce its optimal fit into the binding site (such as **20**, **25**, **30**, and **55**), with the exception of **51**. In the case of **51**, the flexibility of the (hydroxypropyl)-amino side chain may contribute to the tolerance of its 1,2-substitution pattern. Second, the nitrogen position in the upper and lower rings seems to contribute significantly to the binding affinities of different kinases. A subtle change of the nitrogen position may completely change the mode of hydrogen bonding and consequently dramatically alter the selectivity profile of a compound. For example, comparing **8** and **15** (Table 1), the shift of a nitrogen atom from the outer ortho-position to the inner ortho-position, relative to the 3-chloroanilino group, changes the formation of the hydrogen bond from **8** with Leu83 of CDK1 to **15** with Cys1045 of VEGFR-2, therefore giving them different selectivity at CDK1 versus VEGFR-2. The addition of the second nitrogen to the lower ring of **15** (such as **38**, Table 2) reduces the basicity of the first outer nitrogen and weakens the strength of its hydrogen bond with Cys919 of VEGFR-2, leading to a decreased potency of **38** at VEGFR-2. Meanwhile, the removal of the first outer nitrogen of the lower ring of **38** (such as **42**) eliminates its hydrogen bond with Cys919 and thus abolishes the VEGFR-2 inhibitory potency of **42**. Compared to **15**, **47** (Table 2) moves the lower pyridine nitrogen from the meta- to the para-position, relative to the pyrazine ring. This change may set the lower nitrogen at a more favorable position to form the hydrogen bond with Lys33 of CDK1 and a less favorable position to form the hydrogen bond with Cys919 of VEGFR-2, therefore restoring some CDK1 inhibitory potency and reducing some VEGFR-2 inhibitory potency at the same time.

Conclusion

Attempts to optimize a CDK1 inhibitor by using palladium-catalyzed C–C bond, C–N bond formation reactions to assemble diverse biheteroaryl molecules led to the unexpected discovery of a pyrazine–pyridine biheteroaryl as a novel potent VEGFR-2 inhibitor. Compound **15**, which had $IC_{50} = 0.084 \mu M$ inhibitory potency at VEGFR-2, showed very modest selectivity against FGFR-2 ($IC_{50} = 0.21 \mu M$), PDGF-R ($IC_{50} = 0.36$

μM), and GSK-3 ($\text{IC}_{50} = 0.478 \mu\text{M}$), while it exhibited more than 10-fold selectivity against EGFR ($\text{IC}_{50} = 1.36 \mu\text{M}$) and insulin-R kinase ($\text{IC}_{50} = 1.69 \mu\text{M}$). On the other hand, compound **15** exhibited more than 100-fold selectivity against calmodulin kinase 2, casein kinase-1 or -2, CDK1, CDK4, MAPK, PKA, PKC β 2, and PKC γ ($\text{IC}_{50} > 10 \mu\text{M}$). Compound **15** also displayed high inhibitory potency at VEGF-stimulated HUVEC and good selectivity against cell lines such as HUVEC, HASMC, and MRC5. Molecular docking studies were conducted in an attempt to rationalize the unexpected high VEGFR-2 selectivity of **15**. The high potency, good kinase selectivity profile, and high cellular potency/selectivity of compound **15** may render it as valuable pharmacological tool in elucidating the complex roles of VEGF signaling pathways and the potential utility for anti-angiogenesis therapy.

Experimental Section

Chemistry. ^1H NMR spectra were measured on a Bruker AC-300 (300 MHz) spectrometer using tetramethylsilane as an internal standard. Elemental analyses were obtained by Quantitative Technologies Inc. (Whitehouse, NJ), and the results were within 0.4% of the calculated values unless otherwise mentioned. Melting points were determined in open capillary tubes with a Thomas-Hoover apparatus and were uncorrected. Electrospray mass spectra (MS-ES) were recorded on a Hewlett-Packard 59987A spectrometer. High-resolution mass spectra (HRMS) were obtained on a Micromass Autospec. E spectrometer. The term "DMAP" refers to (dimethylamino)pyridine, "TFA" refers to trifluoroacetic acid, "NMP" refers to 1-methyl-2-pyrrolidinone, "DPPF" refers to 1,1'-bis(diphenylphosphino)ferrocene, "Pd₂(dba)₃" refers to tris(dibenzylideneacetone)dipalladium(0)-chloroform adduct, and "DPPA" refers to diphenylphosphoryl azide.

(3-Chlorophenyl)(6-chloropyrimidin-4-yl)amine 2. A mixture of 4,6-dichloropyrimidine compound **1** (4 g, 26.9 mmol), 3-chloroaniline (3.44 g, 26.9 mmol), palladium acetate (121 mg, 38 mmol), BINAP (368 mg, 59 mmol), and NaO-*t*-Bu (3.61 g, 217 mmol) in toluene (100 mL) was stirred at 90 °C for 40 h under nitrogen. The cooled reaction mixture was concentrated under vacuum. The residue was diluted with dichloromethane and filtered through Celite, the Celite was washed with acetone, and the combined filtrates were concentrated under vacuum. The product was purified by column chromatography (100% dichloromethane as solvent) to give 250 mg (4%) of compound **2** as a solid: ^1H NMR (300 MHz, DMSO-*d*₆) δ 8.56 (s, 1 H), 7.94 (s, 1 H), 7.44 (d, $J = 8.4$ Hz, 1 H), 7.38 (t, $J = 8.0$ Hz, 1 H), 7.12 (d, $J = 8.2$ Hz, 1 H), 6.84 (s, 1 H); MS (ES) m/z 240 (M + H⁺).

(3-Chlorophenyl)(6-chloropyrimidin-4-yl)carbamic Acid tert-Butyl Ester 3. A mixture of compound **2** (240 mg, 1 mmol), Boc₂O (436 mg, 2 mmol), and DMAP (cat.) in CH₂Cl₂ was stirred at 20 °C for 3 h and concentrated. The product was purified by column chromatography (EtOAc/hexane as solvent) to give 308 mg (91%) of compound **3** as an oil: MS (ES) m/z 362 (M + Na). Anal. (C₁₅H₁₅N₃O₂Cl₂) C, H, N.

(5-Bromopyridin-3-yl)carbamic Acid tert-Butyl Ester 5. A mixture of 5-bromonicotinic acid compound **4** (7.14 g, 35.4 mmol), *t*-BuOH (155 mL), triethylamine (6.08 g, 60 mmol), and DPPA (10.69 g, 38.9 mmol) in toluene (115 mL) was stirred at 65 °C for 30 min then warmed to 95 °C for 15 h under nitrogen. The cooled reaction mixture was concentrated under vacuum. The product was purified by column chromatography (SiO₂, ethyl acetate/hexane as solvent) to give 2.9 g (30%) of compound **5** as a white solid: ^1H NMR (300 MHz, CDCl₃) δ 8.32 (m, 3 H), 6.97 (brs, 1 H), 1.53 (s, 9 H); MS (ES) m/z 273, 275 (M + H⁺). Anal. (C₁₀H₁₃N₂O₂Br) C, H, N.

(5-Bromopyridin-3-yl)[3-(tert-butyltrimethylsilyl)oxypropyl]carbamic Acid tert-Butyl Ester 6. A mixture

of compound **5** (2.85 g, 10.44 mmol), (3-bromopropoxy)-*tert*-butyldimethylsilane (3.96 g, 15.66 mmol), and Cs₂CO₃ (10.21 g, 31.3 mmol), in anhydrous DMF (55 mL), was stirred at 70 °C for 23 h under nitrogen. The cooled reaction mixture was diluted with water and extracted with ether (3 \times), dried (Na₂SO₄), and concentrated. The product was purified by column chromatography (EtOAc/hexane as solvent) to give 4.2 g (90%) of compound **6** as yellow oil: ^1H NMR (300 MHz, CDCl₃) δ 8.45 (brs, 2 H), 7.77 (brs, 1 H), 3.73 (brt, $J = 7.3$ Hz, 2 H), 3.62 (t, $J = 5.9$ Hz, 2 H), 1.81 (m, 2 H), 1.45 (s, 9 H), 0.84 (s, 9 H), 0.00 (s, 6 H); MS (ES) m/z 445, 447 (M + H⁺). Anal. (C₁₉H₃₃N₂O₃BrSi) C, H, N.

[3-(tert-Butyldimethylsilyl)oxypropyl](5-(tributylstannanyl)pyridin-3-yl)carbamic Acid tert-Butyl Ester 7. A mixture of compound **6** (500 mg, 1.12 mmol), bis-(tributyltin) (780 mg, 1.345 mmol), tri-*o*-tolylphosphine (88.5 mg, 0.29 mmol), palladium acetate (11.3 mg, 0.05 mmol), triethylamine (226 mg, 2.24 mmol) in acetonitrile was stirred at 95–100 °C for 23 h under nitrogen. The cooled reaction mixture was concentrated, sodium carbonate solution was added, and the mixture stirred for 10 min before being extracted with hexane (4 \times). The combined hexane was filtered through Celite, dried (Na₂SO₄), and concentrated. The product was purified by column chromatography (EtOAc/hexane as solvent) to give 395 mg (54%) of compound **7** as an oil: ^1H NMR (300 MHz, CDCl₃) δ 8.39 (d, $J = 1.2$ Hz, 1 H), 8.37 (m, 1 H), 7.55 (m, 1 H), 3.72 (brt, $J = 7.3$ Hz, 2 H), 3.63 (t, $J = 6.2$ Hz, 2 H), 1.89–1.10 (m, 29 H), 0.89 (t, $J = 7.2$ Hz, 9 H), 0.85 (s, 9 H), 0.00 (s, 6 H); MS (ES) m/z 657 (M + H⁺).

3-[[5-[6-(3-Chlorophenyl)amino]pyrimidin-4-yl]pyridin-3-yl]amino]propan-1-ol 8. A mixture of compound **7** (396 mg, 0.6 mmol), compound **3** (293 mg, 0.86 mmol), Pd₂(dba)₃ (16 mg, 0.015 mmol), and triphenylarsine (37 mg, 0.12 mmol) in THF (8 mL) was refluxed for 41 h under nitrogen. The reaction mixture was concentrated, sodium carbonate solution was added, and the mixture stirred for 10 min before being extracted with ether (3 \times). The combined ether layer was dried (Na₂SO₄) and concentrated. The product was purified by column chromatography (EtOAc/hexane as solvent) to give 63 mg (16%) of the silylated product as an oil: MS (ES) m/z 670 (M + H⁺).

The silylated product was dissolved in TFA (2 mL) and stirred at room temperature for 5 h before it was concentrated. An ammonium hydroxide solution was added to the solution until the pH was about 10–11, water was added, and a yellow solid was formed. The yellow solid was collected through filtration, washed with more water, and dried under vacuum. The yellow solid was purified by column chromatography (dry loading, methylene chloride/methanol as solvent) to give 26 mg (77%) of compound **8** as yellow solid: ^1H NMR (300 MHz, DMSO-*d*₆) δ 9.94 (s, 1 H), 8.79 (s, 1 H), 8.36 (s, 1 H), 8.08 (brs, 2 H), 7.56 (d, $J = 9.2$ Hz, 1 H), 7.47 (s, 1 H), 7.37 (t, $J = 8.1$ Hz, 1 H), 7.24 (s, 1 H), 7.07 (d, $J = 7.8$ Hz, 1 H), 6.14 (m, 1 H), 4.55 (t, $J = 5$ Hz, 1 H), 3.53 (m, 2 H), 3.17 (m, 2 H), 1.75 (m, 2 H); MS (ES) m/z 356 (M + H⁺). Anal. (C₁₈H₁₈N₅OCl \cdot 0.2H₂O) C, H, N.

5-(Tributylstannanyl)nicotinic Acid Ethyl Ester 10. A mixture of 5-bromonicotinate **9** (25 g, 108.7 mmol), bis-(tributyltin) (63.05 g, 108.7 mmol), palladium acetate (1.1 g, 4.89 mmol), tri-*o*-tolylphosphine (8.6 g, 28.26 mmol), and triethylamine (21.96 g, 217.4 mmol) in acetonitrile (350 mL) was stirred at 95–100 °C for 22 h under nitrogen. The cooled reaction mixture was filtered through Celite. Then the Celite was washed with more acetonitrile and the combined acetonitrile was concentrated under vacuum. The residue was diluted with a suitable solvent, such as dichloromethane, washed with aqueous sodium carbonate, and concentrated. The residue was further diluted with hexane. The solid was filtered off and the filtrate was concentrated. The product was purified by column chromatography (twice, SiO₂, dichloromethane/hexane as solvent) to give 19.09 g (40%) of **10** as a light orange oil: ^1H NMR (300 MHz, CDCl₃) δ 9.11 (brs, 1 H), 8.74 (brs, 1 H), 8.35 (brs, 1 H), 4.41 (q, $J = 6.9$ Hz, 2 H), 1.72–1.05 (m, 21 H), 0.89 (t, $J = 7.2$ Hz, 9 H); MS (ES) m/z 442 (M + H⁺).

General Procedure for the Synthesis of 11, 16, 21, and 26. 5-(6-Chloropyrazin-2-yl)nicotinic Acid Ethyl Ester 11. A mixture of **10** (10 g, 22.7 mmol), 2, 6-dichloropyrazine (6.76 g, 45.4 mmol), dichlorobis(triphenylphosphine)palladium (797 mg, 1.14 mmol), and LiCl (4.77 g, 113.5 mmol) in anhydrous toluene (85 mL) was stirred at 100 °C for 23 h under nitrogen. The cooled reaction mixture was concentrated under vacuum. Aqueous sodium carbonate was added to the residue, and the mixture stirred for 10 min and was extracted with dichloromethane (3×). The combined dichloromethane solution was filtered through Celite, dried (Na₂SO₄), and concentrated. The product was purified by column chromatography (EtOAc/hexane as solvent) to give 3.56 g (60%) of **11** as an off-white solid: ¹H NMR (300 MHz, CDCl₃) δ 9.43 (brs, 1 H), 9.35 (brs, 1 H), 9.05 (s, 1 H), 8.91 (s, 1 H), 8.64 (s, 1 H), 4.48 (q, *J* = 7.3 Hz, 2 H), 1.47 (t, *J* = 7.2 Hz, 3 H); MS (ES) *m/z* 264 (M + H⁺). Anal. (C₁₂H₁₀N₃O₂Cl) C, H, N.

General Procedure for the Synthesis of 12, 17, 22, and 27. 5-[6-(3-Chlorophenyl)amino]-pyrazin-2-yl]nicotinic Acid Ethyl Ester 12. A mixture of **11** (24.3 g, 92.4 mmol), 3-chloroaniline (16.6 g, 129 mmol), Pd₂(dba)₃ (2.39 g, 2.31 mmol), DPPF (4.1 g, 7.4 mmol), and Cs₂CO₃ (60.2 g, 185 mmol) in anhydrous dioxane (230 mL) was stirred at 110 °C for 46 h under nitrogen. Dichloromethane (100 mL) was added to the cooled reaction mixture. The mixture was then filtered through Celite, the Celite cake was washed with more dichloromethane, and the combined filtrate was concentrated to give a yellow-brown solid. Small amounts of dichloromethane were added, the solid was collected through filtration, and the filtrate was concentrated. The solid collected was recrystallized from EtOAc/hexane to give 21.83 g (67%) of compound **12** as a yellow solid: ¹H NMR (300 MHz, CDCl₃) δ 9.44 (brs, 1 H), 9.31 (brs, 1 H), 8.90 (s, 1 H), 8.57 (s, 1 H), 8.26 (s, 1 H), 7.72 (s, 1 H), 7.44 (d, *J* = 8.1 Hz, 1 H), 7.31 (t, *J* = 8.0 Hz, 1 H), 7.08 (d, *J* = 8.0 Hz, 1 H), 7.04 (s, 1 H), 4.48 (q, *J* = 7.2 Hz, 2 H), 1.46 (t, *J* = 7.0 Hz, 3 H); MS (ES) *m/z* 355 (M + H⁺). Anal. (C₁₈H₁₅N₄O₂Cl) C, H, N.

General Procedure for the Synthesis of 13, 18, 23, and 28. 5-[6-(*tert*-Butoxycarbonyl(3-chlorophenyl)amino)pyrazin-2-yl]nicotinic Acid 13. A mixture of **12** (21.83 g, 61.7 mmol), Boc₂O (26.9 g, 123 mmol), and DMAP (~3 g, cat.) in dichloromethane (500 mL) was stirred at 20 °C for 4 h. The reaction mixture was concentrated and the product was purified by column chromatography (EtOAc/hexane as solvent) to give 26.7 g (95%) of **Boc-13** as yellowish oil: ¹H NMR (300 MHz, CDCl₃) δ 9.22 (d, *J* = 2.0 Hz, 1 H), 9.15 (d, *J* = 2.2 Hz, 1 H), 9.10 (s, 1 H), 8.84 (s, 1 H), 8.64 (t, *J* = 2.1 Hz, 1 H), 7.35 (m, 3 H), 7.18 (brd, *J* = 7.3 Hz, 1 H), 4.44 (q, *J* = 7.1 Hz, 2 H), 1.50 (s, 9 H), 1.44 (t, *J* = 7.1 Hz, 3 H); MS (ES) *m/z* 455 (M + H⁺).

Compound **Boc-13** (32.2 g, 71 mmol) was dissolved in methanol (200 mL) and the mixture was stirred for 10 min and then cooled to 0 °C. A NaOH(aq) (1 N, 118 mL) solution was added slowly and the mixture was stirred at 0 °C for 20 min then stirred at 20 °C for another 18 h. Glacial acetic acid (95 mL) was added to the reaction mixture at 0 °C, slowly followed by the addition of water (350 mL). A yellow solid was formed. The yellow solid was collected through filtration, washed with water (5×), and dried in a vacuum oven overnight to give 28.3 g (94%) of the carboxylic acid **13** as a yellow solid: ¹H NMR (300 MHz, DMSO-*d*₆) δ 9.27 (d, *J* = 1.9 Hz, 1 H), 9.22 (s, 1 H), 9.09 (d, *J* = 1.6 Hz, 1 H), 9.03 (s, 1 H), 8.65 (brs, 1 H), 7.52–7.31 (m, 4 H), 1.44 (s, 9 H); MS (ES) *m/z* 425 (M + H⁺). Anal. (C₂₁H₁₉N₄O₄Cl) C, H, N.

General Procedure for the Synthesis of 14, 19, 24, and 29. [6-(5-(*tert*-Butoxycarbonyl)amino)pyridin-3-yl]pyrazin-2-yl(3-chlorophenyl)carbamate Acid *tert*-Butyl Ester 14. A mixture of the carboxylic acid **13** (28.3 g, 66.5 mmol), DPPA (21.95 g, 80 mmol), triethylamine (13.43 g, 133 mmol), and *t*-BuOH (280 mL) in toluene (200 mL) was stirred under nitrogen at 70 °C for 30 min and then stirred at 100 °C for 4 h. The reaction mixture was concentrated under vacuum. The product was purified by column chromatography (EtOAc/

hexane as solvent) to give 29.28 g (89%) of **14** as a yellowish foam: ¹H NMR (300 MHz, CDCl₃) δ 8.99 (s, 1 H), 8.80 (s, 1 H), 8.67 (d, *J* = 1.7 Hz, 1 H), 8.49 (d, *J* = 2.4 Hz, 1 H), 8.41 (brs, 1 H), 7.29 (m, 3 H), 7.17 (d, *J* = 7.5 Hz, 1 H), 7.08 (s, 1 H), 1.54 (s, 9 H), 1.49 (s, 9 H); MS (ES) *m/z* 498 (M + H⁺). Anal. (C₂₅H₂₈N₅O₄Cl) C, H, N.

General Procedure for the Synthesis of 15, 20, 25, and 30. 3-[5-[6-(3-chlorophenyl)amino]pyrazinyl]-3-pyridin-yl]amino]-1-propanol 15. A mixture of **14** (3 g, 6 mmol), (3-bromopropoxy)-*tert*-butyldimethylsilane (2.28 g, 9 mmol), and Cs₂CO₃ (5.9 g, 18 mmol) in DMF (60 mL) was stirred at 70 °C under nitrogen for 36 h. The reaction mixture was diluted with water, extracted with ether (3×), dried (Na₂SO₄), and concentrated. The product was purified by column chromatography (EtOAc/hexane as solvent) to give 3.04 g of the silylated product as orange oil. The silylated product was dissolved in TFA (30 mL) and stirred for 1 h before it was concentrated. An ammonium hydroxide solution was added to the residue until the pH was about 10–11, water was added, and a yellow solid was formed. The yellow solid was collected through filtration, washed with water, and dried under vacuum. The yellow solid was recrystallized from CH₃OH/EtOAc to give 1.25 g (59%) of **15** as a light yellow solid: ¹H NMR (300 MHz, CD₃OD) δ 8.45 (s, 1 H), 8.41 (d, *J* = 1.6 Hz, 1 H), 8.12 (brs, 2 H), 8.00 (d, *J* = 2.7 Hz, 1 H), 7.66 (brs, 1 H), 7.55 (d, *J* = 8.3 Hz, 1 H), 7.30 (t, *J* = 8.1 Hz, 1 H), 6.99 (d, *J* = 7.9 Hz, 1 H), 3.72 (t, *J* = 6.3 Hz, 2 H), 3.33 (t, *J* = 6.8 Hz, 2 H), 1.91 (m, 2 H); MS (ES) *m/z* 356 (M + H⁺). Anal. (C₁₈H₁₈N₅OCl·0.5H₂O) C, H, N.

5-(5-Chloropyrazin-2-yl)nicotinic Acid Ethyl Ester 16. Replacing 2,6-dichloropyrazine with 2,5-dichloropyrazine and following the same procedure as in the preparation of **11** gave **16** as an off-white solid: 54% yield; ¹H NMR (300 MHz, CDCl₃) δ 9.33 (d, *J* = 2.0 Hz, 1 H), 9.23 (d, *J* = 2.2 Hz, 1 H), 8.77 (t, *J* = 2.1 Hz, 1 H), 8.67 (d, *J* = 2.4 Hz, 1 H), 8.45 (d, *J* = 2.4 Hz, 1 H), 4.46 (q, *J* = 7.1 Hz, 2 H), 1.44 (t, *J* = 7.1 Hz, 3 H); MS (ES) *m/z* 264 (M + H⁺). Anal. (C₁₂H₁₀N₃O₂Cl) C, H, N.

5-[5-(3-Chloro-phenylamino)pyrazin-2-yl]nicotinic Acid Ethyl Ester 17. Replacing **11** with **16** and following the same procedure as in the preparation of **12** gave **17** as an off-white solid: 55% yield; ¹H NMR (300 MHz, CDCl₃) δ 9.31 (d, *J* = 2.0 Hz, 1 H), 9.13 (d, *J* = 2.2 Hz, 1 H), 8.65 (t, *J* = 2.1 Hz, 1 H), 8.22 (m, 2 H), 7.67 (brs, 1 H), 7.26 (m, 2 H), 7.04 (m, 1 H), 6.63 (s, 1 H), 4.45 (q, *J* = 7.1 Hz, 2 H), 1.43 (t, *J* = 7.1 Hz, 3 H); MS (ES) *m/z* 355 (M + H⁺). Anal. (C₁₈H₁₅N₄O₂Cl) C, H, N.

5-[5-(*tert*-Butoxycarbonyl(3-chlorophenyl)amino)pyrazin-2-yl]nicotinic acid 18. Replacing **12** with **17** and following the same procedure as in the preparation of **13** gave **18** as an off-white solid: 55% yield; MS (ES) *m/z* 425 (M + H⁺).

[5-(5-(*tert*-Butoxycarbonyl)amino)pyridin-3-yl]pyrazin-2-yl(3-chlorophenyl)carbamate Acid *tert*-Butyl Ester 19. Replacing **13** with **18** and following the same procedure as in the preparation of **14** gave **19** as a white foam: 74% yield; ¹H NMR (300 MHz, CDCl₃) δ 8.64 (d, *J* = 2.1 Hz, 2 H), 8.54 (d, *J* = 2.5 Hz, 1 H), 8.50 (d, *J* = 2.3 Hz, 1 H), 8.31 (brs, 1 H), 7.26–7.00 (m, 4 H), 6.57 (s, 1 H), 1.52 (s, 9 H), 1.27 (s, 9 H); MS (ES) *m/z* 498 (M + H⁺). Anal. (C₂₅H₂₈N₅O₄Cl) C, H, N.

3-[5-[5-(3-chlorophenyl)amino]pyrazinyl]-3-pyridin-yl]amino]-1-propanol 20. Replacing **14** with **19** and following the same procedure as in the preparation of **15** gave **20** as a light yellow oil: 51% yield; ¹H NMR (300 MHz, CDCl₃) δ 8.15 (brs, 2 H), 8.08 (d, *J* = 2.6 Hz, 1 H), 7.97 (d, *J* = 2.6 Hz, 1 H), 7.72 (brs, 1 H), 7.33 (d, *J* = 8.2 Hz, 1 H), 7.20 (m, 2 H), 7.09 (brs, 1 H), 6.99 (d, *J* = 7.9 Hz, 1 H), 4.57 (m, 1 H), 3.77 (t, *J* = 5.6 Hz, 2 H), 3.27 (m, 2 H), 1.86 (m, 2 H); MS (ES) *m/z* 356 (M + H⁺). Anal. (C₁₈H₁₈N₅OCl·0.2H₂O) C, H, N.

5-(5-Bromopyrimidin-2-yl)nicotinic Acid Ethyl Ester 21. Replacing 2,6-dichloropyrazine with 5-bromo-2-iodopyrimidine and following the same procedure as in the preparation of **11** gave **21** as a yellow solid: 18% yield; ¹H NMR (300 MHz, CDCl₃) δ 9.76 (d, *J* = 2.1 Hz, 1 H), 9.33 (d, *J* = 2.0 Hz, 1 H), 9.24 (t, *J* = 2.1 Hz, 1 H), 8.91 (s, 2 H), 4.46 (q, *J* = 7.1 Hz, 2 H), 1.45 (t, *J* = 7.1 Hz, 3 H); MS (ES) *m/z* 310 (M + H⁺).

5-[5-(3-Chlorophenyl)amino]pyrimidin-2-yl]nicotinic Acid Ethyl Ester 22. Replacing **16** with **21** and following the same procedure as in the preparation of **17** gave **22** as a light yellow solid: 27% yield; $^1\text{H NMR}$ (300 MHz, CDCl_3) δ 9.71 (d, $J = 2.1$ Hz, 1 H), 9.27 (d, $J = 2.0$ Hz, 1 H), 9.19 (t, $J = 2.1$ Hz, 1 H), 8.66 (s, 2 H), 7.29 (m, 1 H), 7.15 (t, $J = 1.9$ Hz, 1 H), 7.04 (m, 2 H), 5.90 (s, 1 H), 4.46 (q, $J = 7.1$ Hz, 2 H), 1.45 (t, $J = 7.1$ Hz, 3 H); MS (ES) m/z 355 (M + H⁺).

5-[5-[(tert-Butoxycarbonyl)(3-chlorophenyl)amino]pyrimidin-2-yl]nicotinic Acid 23. Replacing **17** with **22** and following the same procedure as in the preparation of **18** gave **23** as a yellow solid: 70% yield; MS (ES) m/z 425 (M - H⁺).

[2-(5-[(tert-Butoxycarbonyl)amino]pyridin-3-yl)pyrimidin-5-yl](3-chlorophenyl)carbamic Acid tert-Butyl Ester 24. Replacing **18** with **23** and following the same procedure as in the preparation of **19** gave **24** as a yellow foam: 76% yield; $^1\text{H NMR}$ (300 MHz, CDCl_3) δ 9.28 (d, $J = 1.7$ Hz, 1 H), 8.90 (s, 1 H), 8.67 (s, 2 H), 8.65 (brs, 1 H), 7.41–7.12 (m, 5 H), 1.55 (s, 9 H), 1.50 (s, 9 H); MS (ES) m/z 498 (M + H⁺).

3-[[5-[5-(3-chlorophenyl)amino]-2-pyrimidinyl]-3-pyridinyl]amino]-1-propanol 25. Replacing **19** with **24** and following the same procedure as in the preparation of **20** gave **25** as a yellow foam: 65% yield; $^1\text{H NMR}$ (300 MHz, $\text{DMSO-}d_6$) δ 8.91 (s, 1 H), 8.71 (s, 2 H), 8.64 (brs, 1 H), 8.01 (d, $J = 2.6$ Hz, 1 H), 7.72 (brs, 1 H), 7.31 (t, $J = 8.0$ Hz, 1 H), 7.16 (s, 1 H), 7.14 (d, $J = 8.2$ Hz, 1 H), 6.97 (d, $J = 7.0$ Hz, 1 H), 6.04 (t, $J = 5.3$ Hz, 1 H), 4.55 (t, $J = 5.1$ Hz, 1 H), 3.53 (q, $J = 5.4$ Hz, 2 H), 3.14 (q, $J = 5.9$ Hz, 2 H), 1.74 (m, 2 H); MS (ES) m/z 356 (M + H⁺). Anal. ($\text{C}_{18}\text{H}_{18}\text{N}_5\text{OCl}\cdot 0.5\text{H}_2\text{O}$) C, H, N.

5-(5-Bromopyrimidin-4-yl)nicotinic Acid Ethyl Ester 26. Replacing 2,6-dichloropyrazine with 4-chloro-5-bromopyrimidine and following the same procedure as in the preparation of **11** gave **26** as an off-white solid: 16% yield; $^1\text{H NMR}$ (300 MHz, CDCl_3) δ 9.35 (d, $J = 2.0$ Hz, 1 H), 9.24 (m, 2 H), 9.00 (s, 1 H), 8.78 (t, $J = 2.1$ Hz, 1 H), 4.46 (q, $J = 7.1$ Hz, 2 H), 1.44 (t, $J = 7.1$ Hz, 3 H); MS (ES) m/z 310 (M + H⁺). Anal. ($\text{C}_{12}\text{H}_{10}\text{N}_3\text{O}_2\text{Br}$) C, H, N.

5-[5-(3-Chlorophenyl)amino]pyrimidin-4-yl]nicotinic Acid Ethyl Ester 27. Replacing **21** with **26** and following the same procedure as in the preparation of **22** gave **27** as a yellow-brown foam: 84% yield; $^1\text{H NMR}$ (300 MHz, CDCl_3) δ 9.14 (brs, 2 H), 8.97 (d, $J = 1.3$ Hz, 1 H), 8.79 (s, 1 H), 8.67 (d, $J = 1.5$ Hz, 1 H), 7.19 (t, $J = 8.4$ Hz, 1 H), 6.99 (m, 2 H), 6.86 (brd, $J = 8.0$ Hz, 1 H), 6.21 (brs, 1 H), 4.40 (q, $J = 7.1$ Hz, 2 H), 1.40 (t, $J = 7.1$ Hz, 3 H); MS (ES) m/z 355 (M + H⁺).

5-[5-[(tert-Butoxycarbonyl)(3-chlorophenyl)amino]pyrimidin-4-yl]nicotinic Acid 28. Replacing **22** with **27** and following the same procedure as in the preparation of **23** gave **28** as a yellow solid: 92% yield; $^1\text{H NMR}$ (300 MHz, CDCl_3) δ 9.35 (d, $J = 1.7$ Hz, 1 H), 9.28 (s, 1 H), 9.18 (d, $J = 2.1$ Hz, 1 H), 8.78 (s, 1 H), 8.72 (t, $J = 2.0$ Hz, 1 H), 7.11 (m, 3 H), 6.90 (brd, $J = 7.4$ Hz, 1 H), 1.35 (s, 9 H); MS (ES) m/z 425 (M - H⁺).

[4-(5-[(tert-Butoxycarbonyl)amino]pyridin-3-yl)pyrimidin-5-yl](3-chlorophenyl)carbamic Acid tert-Butyl Ester 29. Replacing **23** with **28** and following the same procedure as in the preparation of **24** gave **29** as a yellowish foam: 81% yield; $^1\text{H NMR}$ (300 MHz, CDCl_3) δ 9.22 (s, 1 H), 8.70 (s, 1 H), 8.58 (d, $J = 1.9$ Hz, 1 H), 8.52 (d, $J = 2.4$ Hz, 1 H), 8.34 (brs, 1 H), 7.16 (m, 3 H), 6.90 (d, $J = 7.9$ Hz, 1 H), 6.69 (s, 1 H), 1.52 (s, 9 H), 1.34 (s, 9 H); MS (ES) m/z 498 (M + H⁺). Anal. ($\text{C}_{25}\text{H}_{28}\text{N}_5\text{O}_4\text{Cl}$) C, H, N.

3-[[5-[5-(3-Chlorophenyl)amino]-4-pyrimidinyl]-3-pyridinyl]amino]-1-propanol 30. Replacing **24** with **29** and following the same procedure as in the preparation of **25** gave **30** as a yellow solid: 51% yield; $^1\text{H NMR}$ (300 MHz, CD_3OD) δ 8.88 (s, 1 H), 8.75 (s, 1 H), 8.22 (d, $J = 1.6$ Hz, 1 H), 7.97 (d, $J = 2.7$ Hz, 1 H), 7.18 (m, 2 H), 7.03 (m, 2 H), 6.90 (dd, $J = 7.7, 1.5$ Hz, 1 H), 6.24 (s, 1 H), 4.40 (brt, $J = 5.1$ Hz, 1 H), 3.79 (t, $J = 5.7$ Hz, 2 H), 3.27 (q, $J = 5.7$ Hz, 2 H), 1.88 (m, 2 H); MS (ES) m/z 356 (M + H⁺). Anal. ($\text{C}_{18}\text{H}_{18}\text{N}_5\text{OCl}\cdot 0.4\text{H}_2\text{O}$) C, H, N.

(3-Chlorophenyl)(6-chloropyrazin-2-yl)amine 32. Palladium acetate (0.121 g, 0.537 mmol), BINAP (0.368 g 0.591

mmol), *t*-BuONa (3.609 g, 37.6 mmol), 2,6-dichloropyrazine (4 g, 26.85 mmol), and 3-chloroaniline (3.44 g, 26.85 mmol) in toluene (100 mL) were stirred at 80 °C for 22 h under N_2 . CH_2Cl_2 was added, the reaction mixture was filtered through Celite, and the solvent was evaporated. Product was purified by column chromatography (EtOAc/hexane as solvent) to give 5.8 g (90%) of **32**: $^1\text{H NMR}$ (300 MHz, CDCl_3) δ 8.11 (s, 1 H), 8.03 (s, 1 H), 7.49 (s, 1 H), 7.30 (m, 2 H), 7.12 (m, 1 H), 6.60 (brs, 1 H); MS (ES) m/z 241 (M + H⁺). Anal. ($\text{C}_{10}\text{H}_7\text{N}_3\text{Cl}\cdot 0.13\text{H}_2\text{O}$) C, H, N.

(3-Chlorophenyl)(6-chloropyrazin-2-yl)carbamic Acid tert-Butyl Ester 33. A mixture of **32** (1.1 g, 4.6 mmol), Boc_2O (3 g, 13.8 mmol), and DMAP (~200 mg, cat) in dichloromethane (65 mL) was stirred at 20 °C for 16 h. The reaction mixture was concentrated, and the product was purified by column chromatography (EtOAc/hexane as solvent) to give 1.6 g (100%) of **33** as a tan wax: $^1\text{H NMR}$ (300 MHz, CDCl_3) δ 8.87 (s, 1 H), 8.32 (s, 1 H), 7.34–7.27 (m, 2 H), 7.21 (brs, 1 H), 7.10 (dt, $J = 6.9, 2.1$ Hz, 1 H), 1.46 (s, 9 H); MS m/z 362 (M + Na⁺).

6-(Trimethylstannanyl)pyrazine-2-carboxylic Acid Methyl Ester 34. A mixture of methyl 6-chloro-2-pyrazinecarboxylate **34** (4.50 g, 26.1 mmol), bis(trimethyltin) (10.0 g, 30.5 mmol), tetrakis(triphenylphosphine)palladium (1.51 g, 1.31 mmol), LiCl (3.32 g, 78.3 mmol), and 2,6-di-*tert*-butyl-4-methylphenol (0.230 g, 1.04 mmol) in anhydrous 1,4-dioxane (80 mL) was refluxed at 100 °C for 4.5 h under nitrogen. After being cooled to room temperature, the reaction mixture was filtered. The solid was washed with dichloromethane and the filtrate was concentrated and flash chromatographed (ethyl acetate/hexane as solvent) to give 5.60 g (71%) of organostannane **35** as a yellow oil: $^1\text{H NMR}$ (300 MHz, CDCl_3) δ 9.09 (s, 1 H), 8.73 (s, 1 H), 4.02 (s, 3 H), 0.44 (s, 9 H).

6'-[(tert-Butoxycarbonyl)(3-chlorophenyl)amino][2,2']-bipyrazinyl-6-carboxylic Acid Methyl Ester 36. A mixture of **35** (536 mg, 1.78 mmol), compound **33** (666 mg, 1.96 mmol), dichlorobis(triphenylphosphine)palladium (125 mg, 0.178 mmol), and LiCl (230 mg, 5.42 mmol) in anhydrous toluene (15 mL) was stirred at 100 °C for 6.5 h under nitrogen. The cooled reaction mixture was concentrated under vacuum and purified by flash chromatography (EtOAc/hexane as solvent) to give 593 mg (75%) of **36** as an off-white solid: $^1\text{H NMR}$ (300 MHz, CDCl_3) δ 9.40 (s, 1 H), 9.27 (s, 1 H), 9.20 (s, 1 H), 9.17 (s, 1 H), 7.41–7.32 (m, 2 H), 7.29 (m, 1 H), 7.19–7.16 (m, 1 H), 4.07 (s, 3 H), 1.49 (s, 9 H); MS (ES) m/z 464 (M + Na⁺). Anal. ($\text{C}_{21}\text{H}_{20}\text{N}_5\text{O}_4\text{Cl}$) C, H, N.

{6'-[(tert-Butoxycarbonyl)(3-chlorophenyl)amino][2,2']-bipyrazinyl-6-yl}carbamic Acid tert-Butyl Ester 37. Compound **36** (1.31 g, 2.97 mmol) was treated with LiOH (0.110 g, 4.58 mmol) in THF (10 mL) and water (2.5 mL) for 2 h at room temperature. Acetic acid (0.55 mL) was added and the solution was concentrated to about half of the original volume. After the addition of water, some solid formed. The solid was collected through filtration, washed with water, and dried under vacuum overnight to give 1.22 g (96%) of a carboxylic acid as a yellow solid: MS (ES) m/z 450 (M + Na⁺). A mixture of the carboxylic acid (350 mg, 0.819 mmol), DPPA (340 mg, 1.24 mmol), and triethylamine (0.230 mL, 1.65 mmol) in *t*-BuOH (5 mL) and toluene (4 mL) was heated at 60 °C for 30 min and then the temperature was slowly increased to 80 °C for 2 h and 90 °C for 1 h. After concentration, the reaction mixture was purified by flash chromatography (EtOAc/hexane as solvent) to give 278 mg (68%) of **37** as a yellow solid: $^1\text{H NMR}$ (300 MHz, CDCl_3) δ 9.31 (s, 1 H), 9.23 (s, 1 H), 9.16 (s, 1 H), 8.70 (s, 1 H), 7.96 (brs, 1 H), 7.39–7.30 (m, 2 H), 7.27 (m, 1 H), 7.19–7.15 (m, 1 H), 1.57 (s, 9 H), 1.48 (s, 9 H); MS (ES) m/z 521 (M + Na⁺).

3-[[6'-((3-Chlorophenyl)amino)[2,2']bipyrazinyl-6-yl]amino]propan-1-ol 38. A mixture of compound **37** (60 mg, 0.12 mmol), (3-bromopropoxy)-*tert*-butyldimethylsilane (40 mg, 0.16 mmol), and Cs_2CO_3 (80 mg, 0.25 mmol) in dry DMF (1 mL) was heated at 70 °C for 3.5 h. The reaction mixture was concentrated and purified by column chromatography (EtOAc/hexane as solvent) to give 71 mg (88%) of the **Boc**-**38** as an

off-white solid. Anal. Calcd for $C_{33}H_{47}N_6O_5ClSi$: C, 59.04; H, 7.06; N, 12.52. Found: C, 59.24; H, 7.00; N, 12.11.

Boc-38 (250 mg, 0.373 mmol) was dissolved in TFA (4 mL) and the solution was stirred at room temperature for 3 h before concentration. A saturated NH_4OH solution was added to the residue until the mixture was made basic followed by the addition of water. The precipitated solid was collected through filtration, again washed with water, and dried under vacuum. The product was purified by flash chromatography on silica gel (EtOAc/MeOH as solvent) to provide 112 mg (84%) of **38** as a yellow solid: 1H NMR (300 MHz, $DMSO-d_6$) δ 9.89 (s, 1 H), 8.79 (s, 1 H), 8.47 (s, 1 H), 8.28 (s, 1 H), 8.13 (s, 1 H), 8.00 (s, 1 H), 7.62 (d, $J = 8.2$ Hz, 1 H), 7.39 (t, $J = 8.0$ Hz, 1 H), 7.29 (m, 1 H), 7.04 (d, $J = 8.1$ Hz, 1 H), 4.51 (brs, 1 H), 3.53 (m, 2 H), 3.47–3.41 (m, 2 H), 1.82–1.73 (m, 2 H); MS (ES) m/z 357 (M + H^+); FAB-HRMS (M + H^+) calcd for $C_{17}H_{18}N_6OCl$ 357.1230, found 357.1215.

(6-Bromopyridin-2-yl)[3-(tert-butyldimethylsiloxy)propyl]carbamic Acid tert-Butyl Ester 40. A mixture of 2-amino-6-bromopyridine compound **39** (3.46 g, 20.0 mmol), di-*tert*-butyl dicarbonate (4.80 g, 22.0 mmol), and 4-(dimethylamino)pyridine (0.244 g, 2 mmol) in *t*-BuOH (50 mL) was stirred at room temperature for more than 24 h. The solution was concentrated and purified by flash chromatography (EtOAc/hexane as solvent) to give 1.36 g (25%) of **Boc-39** as clear crystals: 1H NMR (300 MHz, $CDCl_3$) δ 7.88 (d, $J = 8.2$ Hz, 1 H), 7.50 (t, $J = 8.0$ Hz, 1 H), 7.22 (brs, 1 H), 7.12 (d, $J = 7.7$ Hz, 1 H), 1.51 (s, 9 H).

(3-Bromopropoxy)-*tert*-butyldimethylsilane (1.50 g, 5.93 mmol) and CS_2CO_3 (2.43 g, 7.46 mmol) were added to the solution of **Boc-39** in dry DMF (20 mL). After stirring at 70 °C for 18 h, the solvent was evaporated under reduced pressure and the residue was purified by column chromatography (EtOAc/hexane) to provide 1.93 g (88%) of compound **40** as a clear oil: 1H NMR (300 MHz, $CDCl_3$) δ 7.66 (d, $J = 8.2$ Hz, 1 H), 7.44 (m, 1 H), 7.15 (d, $J = 7.6$ Hz, 1 H), 3.99 (t, $J = 7.3$ Hz, 2 H), 3.67 (t, $J = 6.4$ Hz, 2 H), 1.86 (m, 2 H), 1.51 (s, 9 H), 0.88 (s, 9 H), 0.03 (s, 6 H); MS (ES) m/z 467 (M + Na^+). Anal. ($C_{19}H_{33}N_2O_3BrSi$) C, H, N.

[3-(tert-Butyldimethylsiloxy)propyl](6-(tributylstannanyl)pyridin-2-yl)carbamic Acid tert-Butyl Ester 41. A mixture of compound **40** (150 mg, 0.337 mmol), bis(tributyltin) (0.340 mL, 0.673 mmol), tetrakis(triphenylphosphine)palladium (40 mg, 0.035 mmol), LiCl (43 mg, 1.0 mmol), and 2,6-di-*tert*-butyl-4-methylphenol (3 mg, 0.014 mmol) in anhydrous 1,4-dioxane (3 mL) was refluxed at 100 °C for 4 h under nitrogen. The solvent was removed under reduced pressure and the residue was chromatographed over silica gel (ethyl acetate/hexane as solvent) to give 152 mg (69%) of **41** as a clear oil: 1H NMR (300 MHz, $CDCl_3$) δ 7.49 (d, $J = 8.5$ Hz, 1 H), 7.42 (m, 1 H), 7.08 (d, $J = 7.7$ Hz, 1 H), 4.03 (t, $J = 7.3$ Hz, 2 H), 3.65 (t, $J = 6.6$ Hz, 2 H), 1.88 (m, 2 H), 1.61–1.50 (m, 6 H), 1.52 (s, 9 H), 1.37–1.26 (m, 6 H), 1.10–1.05 (m, 6 H), 0.88 (t, $J = 7.4$ Hz, 9 H), 0.87 (s, 9 H), 0.02 (s, 6 H); MS (ES) m/z 656 (M + H^+).

3-{[6-[6-(3-Chlorophenyl)amino]pyrazin-2-yl]pyridin-2-yl}amino}propan-1-ol 42. A mixture of compound **41** (103 mg, 0.157 mmol), *N*-(*tert*-butoxycarbonyl)-*N*-(3-chlorophenyl)-2-amino-6-chloropyrazine **33** (61 mg, 0.18 mmol), dichlorobis(triphenylphosphine)palladium (13 mg, 0.018 mmol), and LiCl (23 mg, 0.54 mmol) in anhydrous toluene (3 mL) was stirred at 100 °C for 3 h under nitrogen. The cooled reaction mixture was concentrated under vacuum and purified by flash chromatography (EtOAc/hexane as solvent) to give 63 mg (62%) of **Boc-42** as a yellow oil: 1H NMR (300 MHz, $CDCl_3$) δ 9.29 (s, 1 H), 8.93 (s, 1 H), 7.73 (dd, $J = 7.8, 1.3$ Hz, 1 H), 7.65 (m, 1 H), 7.61–7.58 (m, 1 H), 7.37–7.28 (m, 3 H), 7.19–7.15 (m, 1 H), 4.12 (t, $J = 7.4$ Hz, 2 H), 3.71 (t, $J = 6.2$ Hz, 2 H), 2.01–1.92 (m, 2 H), 1.53 (s, 9 H), 1.49 (s, 9 H), 0.85 (s, 9 H), 0.02 (s, 6 H); MS (ES) m/z 692 (M + Na^+).

Boc-42 (53 mg, 0.079 mmol) was dissolved in TFA (1.5 mL) and the solution was stirred at room temperature for 2 h before concentration. A saturated NH_4OH solution was added to the residue until the mixture was made basic followed by the

addition of water. The precipitated solid was collected through filtration, washed with water and Et_2O , and dried under vacuum to provide 28 mg (100%) of **42** as a yellow solid: 1H NMR (300 MHz, $DMSO-d_6$) δ 9.80 (s, 1 H), 8.85 (s, 1 H), 8.24 (s, 1 H), 8.12 (s, 1 H), 7.64 (d, $J = 8.1$ Hz, 1 H), 7.56 (m, 1 H), 7.40–7.35 (m, 2 H), 7.02 (d, $J = 7.7$ Hz, 1 H), 6.71 (brs, 1 H), 6.57 (d, $J = 8.3$ Hz, 1 H), 4.48 (brs, 1 H), 3.53 (t, $J = 6.3$ Hz, 2 H), 3.40 (m, 2 H), 1.76 (m, 2 H); MS (ES) m/z 356 (M + H^+). Anal. ($C_{18}H_{18}N_5OCl \cdot 0.55H_2O$) C, H, N.

(4-Iodopyridin-2-yl)carbamic Acid tert-Butyl Ester 44. A mixture of 4-iodopicolinic acid **43** (1.00 g, 3.30 mmol), DPPA (1.36 g, 4.95 mmol), triethylamine (1.4 mL, 10 mmol) in *t*-BuOH (5.5 mL), and toluene (5 mL) was heated at 65 °C for 1.5 h and then 100 °C for 4 h. After concentration, the reaction mixture was purified by flash chromatography (EtOAc/hexane as solvent) to give 515 mg (50%) of **44** as a white solid: 1H NMR (300 MHz, $CDCl_3$) δ 9.17 (brs, 1 H), 8.48 (s, 1 H), 7.98 (dd, $J = 5.2, 1.5$ Hz, 1 H), 7.34 (dd, $J = 5.2, 1.3$ Hz, 1 H), 1.56 (s, 9 H). MS (ES) m/z 343 (M + Na^+).

[3-(tert-Butyldimethylsiloxy)propyl](4-iodopyridin-2-yl)carbamic Acid tert-Butyl Ester 45. A mixture of compound **44** (330 mg, 1.03 mmol), (3-bromopropoxy)-*tert*-butyldimethylsilane (340 mg, 1.34 mmol), and CS_2CO_3 (504 mg, 1.55 mmol) in dry DMF (4 mL) was stirred at 70 °C for 3 h. The solvent was evaporated under reduced pressure and the residue was purified by column chromatography (EtOAc/hexane) to provide 450 mg (89%) of compound **45** as a clear oil: 1H NMR (400 MHz, $CDCl_3$) δ 8.11 (s, 1 H), 8.00 (d, $J = 5.2$ Hz, 1 H), 7.33 (dd, $J = 5.2, 1.3$ Hz, 1 H), 3.99 (t, $J = 7.3$ Hz, 2 H), 3.65 (t, $J = 6.3$ Hz, 2 H), 1.84 (m, 2 H), 1.52 (s, 9 H), 0.87 (s, 9 H), 0.02 (s, 6 H); MS (ES) m/z 515 (M + Na^+).

[3-(tert-Butyldimethylsiloxy)propyl](4-(trimethylstannanyl)pyridin-2-yl)carbamic Acid tert-Butyl Ester 46. A mixture of compound **45** (650 mg, 1.32 mmol), bis(trimethyltin) (870 mg, 2.66 mmol), tetrakis(triphenylphosphine)palladium (150 mg, 0.130 mmol), LiCl (170 mg, 4.00 mmol), and 2,6-di-*tert*-butyl-4-methylphenol (12 mg, 0.054 mmol) in anhydrous 1,4-dioxane (12 mL) was heated at 90 °C for 1.5 h under nitrogen. The solvent was removed under reduced pressure and the residue was chromatographed over silica gel (EtOAc/hexane as solvent) to give 590 mg (84%) of **46** as a clear oil: 1H NMR (300 MHz, $CDCl_3$) δ 8.09 (d, $J = 4.7$ Hz, 1 H), 7.56 (s, 1 H), 7.10 (d, $J = 4.7$ Hz, 1 H), 3.97 (t, $J = 7.2$ Hz, 2 H), 3.64 (t, $J = 6.5$ Hz, 2 H), 1.85 (m, 2 H), 1.49 (s, 9 H), 0.86 (s, 9 H), 0.33 (s, 9 H), 0.00 (s, 6 H); MS (ES) m/z 527 (M + H^+). Anal. ($C_{22}H_{42}N_2O_3SiSn$) C, H, N.

3-{[4-[6-(3-Chlorophenyl)amino]pyrazin-2-yl]pyridin-2-yl}amino}propan-1-ol 47. A mixture of compound **46** (550 mg, 1.04 mmol), compound **33** (360 mg, 1.06 mmol), dichlorobis(triphenylphosphine)palladium (73 mg, 0.104 mmol), and LiCl (132 mg, 3.11 mmol) in anhydrous toluene (20 mL) was stirred at 90 °C for 1 h and then 100 °C for 2 h under nitrogen. The cooled reaction mixture was concentrated under vacuum and purified by flash chromatography (EtOAc/hexane as solvent) to give 380 mg (55%) of **Boc-47** as a yellow oil: 1H NMR (300 MHz, $CDCl_3$) δ 9.00 (s, 1 H), 8.82 (s, 1 H), 8.40 (d, $J = 5.2$ Hz, 1 H), 8.04 (s, 1 H), 7.37–7.28 (m, 4 H), 7.16 (brd, $J = 7.3$ Hz, 1 H), 4.02 (m, 2 H), 3.65 (t, $J = 6.3$ Hz, 2 H), 1.85 (m, 2 H), 1.50 (s, 9 H), 1.49 (s, 9 H), 0.85 (s, 9 H), 0.00 (s, 6 H); MS (ES) m/z 670 (M + H^+).

A solution of **Boc-47** (350 mg, 0.522 mmol) and TFA (4 mL) was left at room temperature overnight before concentration. A saturated NH_4OH solution was added to the residue until the mixture was made basic followed by the addition of water. The precipitated solid was collected through filtration, washed with water, dried under vacuum, and purified by flash chromatography (CH_2Cl_2 /MeOH as solvent) to provide 143 mg (77%) of **47** as a yellow solid: 1H NMR (300 MHz, $DMSO-d_6$) δ 9.88 (s, 1 H), 8.54 (s, 1 H), 8.27 (s, 1 H), 8.10 (d, $J = 5.8$ Hz, 1 H), 8.00 (s, 1 H), 7.73 (d, $J = 8.2$ Hz, 1 H), 7.39 (t, $J = 8.1$ Hz, 1 H), 7.10 (s, 2 H), 7.04 (dd, $J = 7.9, 1.0$ Hz, 1 H), 6.69 (brt, $J = 5.3$ Hz, 1 H), 4.55 (brs, 1 H), 3.51 (t, $J = 6.2$ Hz, 2 H), 3.36 (m, 2 H), 1.73 (m, 2 H); MS (ES) m/z 356 (M + H^+). Anal. ($C_{18}H_{18}N_5OCl \cdot 0.3H_2O$) C, H, N.

(4-(Trimethylstannanyl)pyridin-3-yl)carbamic Acid *tert*-Butyl Ester 49. A mixture of 4-(trimethylstannanyl)nicotinic acid **48** (300 mg, 1.05 mmol), DPPA (433 mg, 1.57 mmol), and triethylamine (0.250 mL, 1.79 mmol) in *t*-BuOH (2 mL) and toluene (2 mL) was heated at 60 °C for 1.5 h and then 90 °C for 3.5 h. After concentration, the reaction mixture was purified by flash chromatography (EtOAc/hexane as solvent) to give 213 mg (57%) of **49** as a white solid: ¹H NMR (300 MHz, CDCl₃) δ 8.54 (s, 1 H), 8.31 (d, *J* = 4.5 Hz, 1 H), 7.34 (d, *J* = 4.5 Hz, 1 H), 6.30 (brs, 1 H), 1.51 (s, 9 H), 0.37 (s, 9 H).

[6-(3-((*tert*-Butoxycarbonyl)amino)pyridin-4-yl)pyrazin-2-yl](3-chlorophenyl)carbamic Acid *tert*-Butyl Ester 50. A mixture of **49** (162 mg, 0.454 mmol), **33** (155 mg, 0.454 mmol), dichlorobis(triphenylphosphine)palladium (64 mg, 0.091 mmol), and LiCl (60 mg, 1.42 mmol) in anhydrous toluene (10 mL) was stirred at 100 °C for 4 h under nitrogen. The reaction mixture was concentrated and purified by flash chromatography (EtOAc/hexane as solvent) to give 156 mg (69%) of **50** as a white solid: ¹H NMR (300 MHz, CDCl₃) δ 9.37 (s, 1 H), 9.23 (s, 1 H), 9.05 (s, 1 H), 8.71 (s, 1 H), 8.37 (d, *J* = 5.1 Hz, 1 H), 7.47–7.27 (m, 3 H), 7.20 (dd, *J* = 7.0, 2.0 Hz, 1 H), 1.56 (s, 9 H), 1.48 (s, 9 H); MS (ES) *m/z* 498 (M + H⁺).

3-{[4-[6-(3-Chlorophenyl)amino]pyrazin-2-yl]pyridin-3-yl}amino]propan-1-ol 51. A mixture of compound **50** (29 mg, 0.058 mmol), (3-bromopropoxy)-*tert*-butyldimethylsilane (22 mg, 0.087 mmol), and Cs₂CO₃ (38 mg, 0.12 mmol) in dry DMF (1 mL) was heated at 70 °C for 2 h. The reaction mixture was concentrated and purified by column chromatography (EtOAc/hexane as solvent) to give 32 mg (82%) of **Boc**₂-**51** as a yellow oil; MS (ES) *m/z* 670 (M + H⁺).

Boc₂-**51** (60 mg, 0.089 mmol) was dissolved in TFA (2 mL) and the solution was stirred at room temperature for 1.5 h before concentration. A saturated NH₄OH solution was added to the residue until the mixture was made basic followed by the addition of water. The precipitated solid was collected through filtration, washed with water, and dried under vacuum. The product was purified by flash chromatography on silica gel (CH₂Cl₂/MeOH as solvent) to provide 28 mg (88%) of **51** as a yellow solid: ¹H NMR (300 MHz, DMSO-*d*₆) δ 9.90 (s, 1 H), 8.51 (s, 1 H), 8.28 (s, 1 H), 8.22 (s, 1 H), 7.95 (brd, *J* = 4.4 Hz, 1 H), 7.83 (s, 1 H), 7.58 (d, *J* = 4.8 Hz, 1 H), 7.51 (d, *J* = 8.5 Hz, 1 H), 7.41 (t, *J* = 8.0 Hz, 1 H), 7.11 (m, 2 H), 4.48 (m, 1 H), 3.37 (m, 2 H), 3.29 (m, 2 H), 1.08 (m, 2 H); MS (ES) *m/z* 356 (M + H⁺). Anal. (C₁₈H₁₈N₅OCl·0.6H₂O) C, H, N.

6-{6-[(*tert*-Butoxycarbonyl)(3-chlorophenyl)amino]pyrazin-2-yl}nicotinic Acid Methyl Ester 53. A mixture of methyl 6-((trifluoromethyl)sulfonyl)oxy)nicotinate **52** (2.00 g, 7.02 mmol), bis(trimethyltin) (3.50 g, 10.7 mmol), tetrakis(triphenylphosphine)palladium (0.810 g, 0.700 mmol), anhydrous LiCl (0.900 g, 21.2 mmol), and 2,6-di-*tert*-butyl-4-methylphenol (0.062 g, 0.28 mmol) in anhydrous 1,4-dioxane (60 mL) was refluxed at 100 °C for 2 h under nitrogen. After being cooled to room temperature, the reaction mixture was filtered through Celite and washed with dichloromethane. The filtrate was concentrated under vacuum. Water and Et₂O were added to the residue and the resulting mixture was filtered again through Celite. The filtrate was separated and the aqueous layer was extracted with Et₂O. The organic layers were combined and washed with 15% NH₄OH (2×), and the aqueous layer was back-extracted with Et₂O. The combined organic phases were dried over Na₂SO₄, filtered, and concentrated to give 2.31 g of crude methyl 6-(trimethylstannanyl)nicotinate as a brown oil.

Compound **33** (2.20 g, 6.47 mmol), dichlorobis(triphenylphosphine)palladium (0.780 g, 1.11 mmol), LiCl (0.900 g, 21.2 mmol), and anhydrous toluene (80 mL) were added to the crude organostannane. The reaction mixture was heated at 100 °C for 1 h under nitrogen and then left at room temperature overnight. After filtration through Celite, the filtrate was concentrated and flash chromatographed (EtOAc/hexane as solvent) to give 1.19 g (38%, two steps) of **53** as a white solid: ¹H NMR (300 MHz, CDCl₃) δ 9.43 (s, 1 H), 9.24 (d, *J* = 2.1 Hz, 1 H), 9.06 (s, 1 H), 8.31 (dd, *J* = 8.3, 2.1 Hz, 1 H), 7.93 (d, *J* = 8.3 Hz, 1 H), 7.39–7.31 (m, 3 H), 7.19–7.15 (m, 1 H), 3.97

(s, 3 H), 1.49 (s, 9 H); MS (ES) *m/z* 463 (M + Na⁺). Anal. (C₂₂H₂₁N₄O₄Cl) C, H, N.

[6-(5-((*tert*-Butoxycarbonyl)amino)pyridin-2-yl)pyrazin-2-yl](3-chlorophenyl)carbamic Acid *tert*-Butyl Ester 54. A mixture of **53** (540 mg, 1.22 mmol) and LiOH (44 mg, 1.8 mmol) in THF (16 mL) and water (4 mL) was stirred for 1 h at room temperature. More LiOH (30 mg, 1.3 mmol) was added to the cloudy solution. After another 3 h at room temperature, the solution became clear. Acetic acid (0.30 mL) was added and the solution was concentrated to about half of the original volume. After the addition of water, some solid formed. The solid was collected through filtration, washed with water, and dried under vacuum overnight to give 522 mg (100%) of a carboxylic acid as a yellow solid: MS (ES) *m/z* 425 (M – H⁺).

A mixture of the carboxylic acid (522 mg, 1.22 mmol), DPPA (500 mg, 1.82 mmol), and triethylamine (0.340 mL, 2.44 mmol) in *t*-BuOH (9 mL) and toluene (9 mL) was heated at 60 °C for 30 min and then the temperature was slowly increased to 80 °C for 2 h and 90 °C for 1 h. After concentration, the reaction mixture was purified by flash chromatography (EtOAc/hexane as solvent) to give 393 mg (65%) of **54** as a yellow solid: ¹H NMR (300 MHz, CDCl₃) δ 9.31 (s, 1 H), 8.92 (s, 1 H), 8.45 (d, *J* = 2.4 Hz, 1 H), 8.03 (brd, *J* = 8.5 Hz, 1 H), 7.84 (d, *J* = 8.6 Hz, 1 H), 7.37–7.29 (m, 3 H), 7.19–7.16 (m, 1 H), 6.67 (s, 1 H), 1.54 (s, 9 H), 1.49 (s, 9 H); MS (ES) *m/z* 520 (M + Na⁺). Anal. (C₂₅H₂₈N₅O₄Cl) C, H, N.

3-{[6-[6-(3-Chlorophenyl)amino]pyrazin-2-yl]pyridin-3-yl}amino]propan-1-ol 55. A mixture of **54** (43 mg, 0.12 mmol), (3-bromopropoxy)-*tert*-butyldimethylsilane (30 mg, 0.12 mmol), and Cs₂CO₃ (45 mg, 0.14 mmol) in dry DMF (1 mL) was heated at 65 °C for 2 h then 80 °C for 2.5 h. The reaction mixture was concentrated and purified by column chromatography (EtOAc/hexane as solvent) to give 51 mg (88%) of **Boc**₂-**55** as a clear oil.

Boc₂-**55** (385 mg, 0.575 mmol) was dissolved in TFA (6 mL) and the solution was stirred at room temperature for 3 h before concentration. A saturated NH₄OH solution was added to the residue until the mixture was made basic, followed by the addition of water. The precipitated solid was collected through filtration, washed with water, and dried under vacuum. The product was purified by flash chromatography on silica gel (CH₂Cl₂/MeOH as solvent) to provide 176 mg (86%) of **55** as a yellow solid: ¹H NMR (300 MHz, DMSO-*d*₆) δ 9.70 (s, 1 H), 8.74 (s, 1 H), 8.11–8.08 (m, 3 H), 7.99 (d, *J* = 8.6 Hz, 1 H), 7.63 (d, *J* = 8.4 Hz, 1 H), 7.37 (t, *J* = 8.1 Hz, 1 H), 7.06 (dd, *J* = 8.6, 2.6 Hz, 1 H), 7.01 (d, *J* = 7.9 Hz, 1 H), 6.37 (m, 1 H), 4.52 (t, *J* = 5.0 Hz, 1 H), 3.53 (m, 2 H), 3.18 (m, 2 H), 1.74 (m, 2 H); MS (ES) *m/z* 356 (M + H⁺). Anal. (C₁₈H₁₈N₅OCl·0.24H₂O) C, H, N.

(5-Bromothiazol-2-yl)carbamic Acid *tert*-Butyl Ester 57. A mixture of (2-amino-5-bromothiazole) **56** (10 g, 38.4 mmol), Boc₂O (8.39 g, 38.4 mmol), DMAP (440 mg, 3.6 mmol), and NaHCO₃ (9.6 g, 114 mmol) in *t*-BuOH (100 mL) was stirred at 20 °C for 16 h. The reaction mixture was concentrated, and the product was purified by column chromatography (EtOAc/hexane as solvent) and recrystallized from ethyl acetate/hexane to give 3.41 g (32%) of **57** as a white solid: ¹H NMR (300 MHz, DMSO-*d*₆) δ 11.70 (brs, 1 H), 7.43 (s, 1 H), 1.48 (s, 9 H). Anal. (C₈H₁₁BrN₂O₂S) C, H, N.

(5-Bromothiazol-2-yl)[3-(*tert*-butyldimethylsiloxy)propyl]carbamic Acid *tert*-Butyl Ester 58. A mixture of compound **57** (2.2 g, 7.91 mmol), (3-bromopropoxy)-*tert*-butyldimethylsilane (3.46 g, 12.7 mmol), and Cs₂CO₃ (7.7 g, 23.7 mmol) in DMF (24 mL) was stirred at 70 °C under nitrogen for 18 h. The reaction mixture was diluted with water, extracted with ether (3×), dried (Na₂SO₄), and concentrated. The product was purified by column chromatography (EtOAc/hexane as solvent) to give 2.6 g (72%) of the silylated product compound **58** as an oil. ¹H NMR (300 MHz, CDCl₃) δ 7.22 (s, 1 H), 4.08 (t, *J* = 7.5 Hz, 2 H), 3.65 (t, *J* = 6.3 Hz, 2 H), 1.85 (m, 2 H), 1.53 (s, 9 H), 0.85 (s, 9 H), 0.01 (s, 6 H). Anal. (C₁₇H₃₁BrN₂O₃SSi) C, H, N.

3-[15-[6-(3-Chlorophenyl)amino]pyrazin-2-yl]thiazol-2-yl]amino]propan-1-ol 59. A mixture of compound **58** (152

mg, 0.337 mmol), bis(tributyltin) (390 mg, 0.34 mmol), tetrakis-(triphenylphosphine)palladium (40 mg, 0.035 mmol), LiCl (43 mg, 1.0 mmol), and BHT (3 mg, 0.014 mmol) in dioxane (3 mL) was stirred at 100 °C for 4 h under nitrogen. The cooled reaction mixture was concentrated under vacuum. The residue was purified by column chromatography (EtOAc/hexane as solvent) to give 56 mg (25%) of organostannane as an oil: ¹H NMR (300 MHz, CDCl₃) δ 7.27 (s, 1 H), 4.15 (t, *J* = 7.4 Hz, 2 H), 3.67 (t, *J* = 6.3 Hz, 2 H), 1.87(m, 2 H), 1.54–1.46 (m, 15 H), 1.28 (m, 6 H), 1.05 (t, *J* = 8.3 Hz, 6 H), 0.85 (m, 18 H), 0.01 (s, 6 H); MS (ES) *m/z* 663 (M + 1⁺).

A mixture of organostannane (140 mg, 0.21 mmol), **33** (72 mg, 0.21 mmol), Pd(PPh₃)₂Cl₂ (15 mg, 0.021 mmol), and LiCl (27 mg, 0.62 mmol) in toluene (3.5 mL) was stirred at 100 °C for 3 h under nitrogen. The cooled reaction mixture was concentrated under vacuum. The residue was purified by column chromatography (EtOAc/hexane as solvent) to give 96 mg (68%) of the **Boc₂-59** as an oil.

Boc₂-59 was dissolved in dichloromethane (2 mL) and TFA (2.6 mL) and stirred at 20 °C for 18 h before concentrated. Ammonium hydroxide solution was added to the residue until the pH was about 10–11 and a yellow solid was formed. The yellow solid was collected through filtration, washed with water, and dried under vacuum to give **59** as a light yellow solid: ¹H NMR (300 MHz, CD₃OD) δ 8.23 (s, 1 H), 8.10 (t, *J* = 2.0 Hz, 1 H), 7.84 (s, 1 H), 7.74 (s, 1 H), 7.45 (dd, *J* = 8.3, 1.3 Hz, 1 H), 7.26 (t, *J* = 8.1 Hz, 1 H), 6.97 (dd, *J* = 7.8, 1.1 Hz, 1 H), 3.68 (t, *J* = 6.2 Hz, 2 H), 3.46 (t, *J* = 6.9 Hz, 2 H), 1.88 (m, 2 H); MS (ES) *m/z* 362 (M + 1⁺). Anal. (C₁₆H₁₆N₅OClS) C, H, N.

(3-Chlorophenyl)(6-oxazol-5-ylpyrazin-2-yl)carbamic Acid tert-Butyl Ester 60. A mixture of **33** (678 mg, 2.0 mmol), oxazole (414 mg, 6.0 mmol), potassium acetate (295 mg, 3.0 mmol), and tetrakis(triphenylphosphine)palladium (115 mg, 0.1 mmol) in DMA (5 mL) was heated at 80 °C for 4 days in a sealed tube. Water was added, the mixture was extracted with CH₂Cl₂, and the extracts were dried (Na₂SO₄) and concentrated. The product was purified by column chromatography (EtOAc/hexane as solvent) to provide 427 mg (57%) of **60** as a white solid: ¹H NMR (300 MHz, CDCl₃) δ 8.92 (s, 1 H), 8.66 (s, 1 H), 7.96 (s, 1 H), 7.43 (s, 1 H), 7.41–7.26 (m, 3 H), 7.14 (d, *J* = 5.0 Hz, 1 H), 1.48 (s, 9 H). Anal. (C₁₈H₁₇ClN₄O₃·0.4H₂O) C, H, N.

(3-Chlorophenyl)[6-(2-iodooxazol-5-yl)pyrazin-2-yl]carbamic Acid tert-Butyl Ester 61. LiHMDS (1.0 M in THF, 1.85 mL, 1.85 mmol) was added to a solution of **60** (288 mg, 0.774 mmol) in THF (7.4 mL) at –78 °C, and the mixture was stirred at –78 °C for 1 h. A solution of 1,2-diiodoethane (492 mg, 1.74 mmol) in THF (4.9 mL) was added at –78 °C, and the mixture was stirred at –78 °C for 1 h, quenched by adding 10% Na₂S₂O₃, and then extracted with CH₂Cl₂. The extracts were dried (Na₂SO₄) and concentrated. The product was purified by column chromatography (EtOAc/hexane as solvent) to provide 252 mg (68%) of **61** as tan solid: ¹H NMR (300 MHz, acetone-*d*₆) δ 9.00 (s, 1 H), 8.72 (s, 1 H), 7.48–7.29 (m, 5 H), 1.47 (s, 9 H); MS (ES) *m/z* 521 (M + Na⁺).

(3-Chlorophenyl){6-[2-(3-hydroxypropyl)amino]oxazol-5-yl]pyrazin-2-yl}carbamic Acid tert-Butyl Ester 62. A mixture of **61** (198 mg, 0.40 mmol) in 3-amino-1-propanol (4 mL) was heated at 100 °C for 18 h. The reaction mixture was cooled to room temperature and EtOAc was added. This solution was washed with water (3×), dried (Na₂SO₄), and concentrated. Recrystallization from EtOAc provided 41 mg (30%) of **62** as a tan solid: ¹H NMR (300 MHz, DMSO-*d*₆) δ 9.75 (s, 1 H), 8.07 (s, 1 H), 8.03 (s, 1 H), 8.00 (s, 1 H), 7.71 (t, *J* = 5.7 Hz, 1 H), 7.63 (dd, *J* = 8.3, 1.0 Hz, 1 H), 7.44 (s, 1 H), 7.35 (t, *J* = 8.0 Hz, 1 H), 7.01 (dd, *J* = 7.1, 1.1 Hz, 1 H), 4.50 (t, *J* = 5.2 Hz, 1 H), 3.49 (m, 2 H), 3.33 (m, 2 H), 1.72 (m, 2 H). Anal. (C₁₆H₁₆ClN₅O₂·1.1H₂O) C, H, N.

Biology. Kinase Activity Assays. A kinase reaction mixture was prepared in 50 mM Tris-Cl (pH 8), 10 mM MgCl₂, 0.1 mM Na₃VO₄, 1 mM DTT, 1% DMSO, 0.25 μM biotinylated peptide substrate, 0.2–0.8 μCi per well [³³P]-γ-ATP [2000–3000 Ci/mmol], and 5 μM ATP in the presence or absence of

test compound and incubated at 30 °C for 1 h in a streptavidin-coated FlashPlate (Perkin-Elmer, Boston, MA). Biotinylated peptide substrates were described as follows:⁴⁹ VEGFR-2 (biotin-KHKKLAEGSAYEEV-amide), calmodulin kinase 2 (biotin-KKALRRQETVDAL-amide), casein kinase-1 (biotin-KRRRAL-S(phospho)VASLPGL-amide), casein kinase-2 (biotin-RREEE-TEEE-amide), CDK1 (biotin-KTPKKAKKPKTPKKAKKL-amide), CDK4 (GST-retinoblastoma protein construct), EGFR (biotin-DRVYIHPF-amide), FGFR-2 (biotin-poly(GT) 4:1), GSK-3 (biotin-KRREILSRRP(phospho)SYR-amide), insulin-R kinase (biotin-TRDIYETDYYRK-amide), MAPK (biotin-APRTPGRR-amide), PDGF-R (biotin-KHKKLAEGSAYEEV-amide), PKA (biotin-GRGTGRRNSI-amide), PKCβ2 (biotin-RFARKGSLRQKNV-amide), and PKCγ (biotin-RFARKGSLRQKNV-amide). Reaction conditions and components varied slightly depending on the protein kinase being assayed. The reaction was terminated by washing with PBS containing 100 mM EDTA, and plates were counted in a scintillation counter. Inhibition of the enzymatic activity due to compound was measured by observing a reduced amount of [³³P]-γ-ATP incorporated into the immobilized peptide relative to untreated controls. Linear regression analysis of the percent of inhibition by test compound was used to calculate IC₅₀ values (GraphPad Prism 3, GraphPad Software, San Diego, CA).

Cell Culture. HUVEC and HASMC cells were obtained from Cascade Biologicals (Portland, OR) and maintained in Media 200 containing low serum growth supplement (Cascade Biologicals). All other cells were obtained from the American Type Culture Collection (Manassas, VA). HeLa, A375, and HCT-116 cells were cultured in minimal essential medium (MEM) with 0.1 mM nonessential amino acids and 1 mM sodium pyruvate supplemented with 2 mM L-glutamine and 10% FCS (Hyclone, Logan, UT). MRC5 were cultured in Eagles MEM and A375 in Dulbecco's modified Eagles medium with 4 mM l-glutamine and 1.5 g/L sodium bicarbonate supplemented with 10% FCS. Cells were maintained at 37 °C plus 5% CO₂ as exponentially growing monolayers.

VEGF-Stimulated HUVEC Proliferation. To evaluate inhibition of VEGF-stimulated proliferation, HUVEC cells were detached with trypsin and seeded into 96-well plates in F-12K medium (Invitrogen, Carlsbad, CA) containing 0.2% heat-inactivated fetal bovine serum. Cells were stimulated with 2 ng/well VEGF (R&D systems) in the presence or absence of test compounds. BrdU was added 24 h after the addition of VEGF and incubated with cells for an additional 20–24 h. BrdU incorporation was quantified using cell proliferation ELISA with BrdU reagents (Roche Biochemicals, Indianapolis, IN).

Cell Proliferation Assay. The ability of test compound to inhibit the proliferation of cell growth was determined by measuring [¹⁴C]thymidine incorporation into primary cells or cell lines derived from carcinomas originating from several tissues. Briefly, cells were trypsinized and seeded into 96-well CytoStar scintillating microplates (Amersham, Piscataway, NJ) in complete medium in a volume of 100 μL. Cells were incubated for 24 h at 37 °C in an atmosphere containing 5% CO₂. Test compound was added, and cells were incubated for 24 more hours. Methyl [¹⁴C]thymidine (Perkin-Elmer, Boston, MA) was diluted in complete medium and 0.2 μCi was added to each well of the CytoStar plate in a volume of 20 μL. The plate was incubated for 24 additional hours in the presence of test compound. Plates were washed twice with 200 μL PBS and [¹⁴C]thymidine incorporation was quantified on a Packard Top Count. IC₅₀ values reported as > 10 indicate that inhibition did not reach 50% of control at the highest dose tested.

Molecular Docking Procedures. The X-ray structure of VEGFR-2 has been determined in the unliganded, phosphorylated form (PDB code 1VR2).⁵⁰ This structure was first added all the missing hydrogen atoms by the modeling program Maestro,⁵¹ followed by the visual inspection to ensure that all the polar/charged residues form the correct hydrogen bonding with their neighbors. Then, it was energy minimized in the aqueous solution using the GB/SA model.⁵² To prevent the unrealistic movement that may be caused by using an implicit

water model, harmonic position constraints of 100 and 10 kJ/(Å²·mol) were applied to the heavy atoms on the protein backbone and side chain, respectively, while all the hydrogen atoms were treated without position constraints. The final structure was used as the target for VEGFR-2 molecular docking studies.

Since no CDK1 X-ray structures are currently available, a model of CDK1, complexed with its ligand purvalanol B, has been built on the basis of the X-ray structure of CDK2/purvalanol B complex (PDB code 1CKP).⁵³ The quality of this model is promised by the following facts: the amino acid sequence of human CDK1 (SWISS-PROT code PO6493) shares high 63% identity and 74% similarity with human CDK2 (SWISS-PROT code P24941); it has only two different residues, Ser84 and Met85, at the ATP-binding site, as compared to CDK2; furthermore, the side chains of these two different residues are extended out of the ATP-binding site and are not directly involved in ligand binding. The homology-modeling program Prime⁵⁴ was used for the model building. The resulting CDK1-purvalanol B complex structure was further optimized by full energy minimization in the aqueous solution using the GB/SA model,⁵² and the final structure was used as the target structure for CDK1 molecular docking studies.

CGP60474 and **15** were docked into the ATP-binding sites of the target structures of CDK1 or VEGFR-2, respectively, using the docking program Glide.⁵⁵ The standard precision (SP) mode of Glide was used to explore the favorable binding poses, which allowed the ligand conformation be flexibly explored while holding the protein as a rigid structure during the docking. The predicted binding modes were determined as the poses with the best Emodel scores.⁵⁶ Each predicted complex structure was then energy-minimized in the aqueous solution using the GB/SA model.⁵² Harmonic position constraints of 100 and 10 kJ/(Å²·mol) were applied to the residues that were more than 12 Å away or within 6–12 Å from any ligand atom, respectively, while the ligand and the residues that are less than 6 Å from it were treated without position constraints.

All the molecular mechanism calculations were done using the program MacroModel⁵⁷ with the OPLS_AA force field.⁵⁸ Polak-Ribiere conjugate gradient method was used for energy minimization, and the derivative convergence criterion was set at 0.05 kJ/(Å·mol).

Acknowledgment. We thank Mary Pat Beavers for calculating the physical properties of some of the compounds.

Supporting Information Available: Elemental analyses data for the compounds synthesized. This material is available free of charge via the Internet at <http://pubs.acs.org>.

References

- Risau, W. Mechanism of angiogenesis. *Nature* **1997**, *386*, 671–674.
- Ribatti, D.; Vacca, A.; Nico, B.; Roncali, L.; Dammacco, F. Postnatal angiogenesis. *Mech. Devel.* **2001**, *100*, 157–163.
- (a) Folkman, J. Anti-angiogenesis: New concept for therapy of solid tumors. *Ann. Surg.* **1972**, *175*, 409–416. (b) Folkman, J. Tumor angiogenesis: Therapeutic implications. *N. Engl. J. Med.* **1971**, *285*, 1182–1186.
- Spranger, J.; Pfeiffer, A. F. New concepts in pathogenesis and treatment of diabetic retinopathy. *Exp. Clin. Endocrinol. Diabetes* **2001**, *109*(Suppl 2), S438–S450.
- Walsh, D. A.; Haywood, L. Angiogenesis: A therapeutic target in arthritis. *Curr. Opin. Investig. Drugs* **2001**, *2*, 1054–1063.
- McLaren, J.; Prentice, A.; Charnock-Jones, D. S.; Millican, S. A.; Muller, K. H.; Sharkey, A. M.; Smith, S. K. Vascular endothelial growth factor is produced by peritoneal fluid macrophages in endometriosis and is regulated by ovarian steroids. *J. Clin. Invest.* **1996**, *98*, 482–489.
- Detmar, M. *Dermatol. Sci.* **2000**, *24*, S78.
- Folkman, J. What is the evidence that tumors are angiogenesis dependent? *J. Natl. Cancer Inst.* **1990**, *82*, 4–6.
- Liotta, L. A.; Steeg, P. S.; Stetler-Stevenson, W. G. Cancer metastasis and angiogenesis: An imbalance of positive and negative regulation. *Cell* **1991**, *64*, 327–336.
- (a) Nugent, M. A.; Iozzo, R. V. Fibroblast growth factor-2. *Int. J. Biochem. Cell. Biol.* **2000**, *32*, 115–120. (b) Carmeliet, P. Mechanisms of angiogenesis and arteriogenesis. *Nat. Med.* **2000**, *6*, 389–395. (c) Davis, S.; Yancopoulos, G. D. The angiopoietins: Yin and yang in angiogenesis. *Curr. Top. Microbiol. Immunol.* **1999**, *237*, 173–185. (d) Lindahl, P.; Bostrom, H.; Karlsson, L.; Hellstrom, M.; Kalen, M.; Betsholtz, C. Role of platelet-derived growth factors in angiogenesis and alveogenesis. *Curr. Top. Pathol.* **1999**, *93*, 27–33.
- (a) Cross, M. J.; Claesson-Welsh, L. FGF and VEGF function in angiogenesis: Signaling pathways, biological responses, and therapeutic inhibition. *Trends Pharm. Sci.* **2001**, *22*, 201–207. (b) McMahon, G. VEGF receptor signaling in tumor angiogenesis. *Oncologist* **2000**, *5*(Suppl 1), 3–10. (c) Ferrara, N.; Davis-Smyth, T. The biology of vascular endothelial growth factor. *Endocr. Rev.* **1997**, *18*, 4–25.
- De Vries, C.; Escobedo, J. A.; Ueno, H.; Houck, K.; Ferrara, N.; Williams, L. T. The fms-like tyrosine kinase, a receptor for vascular endothelial growth factor. *Science* **1992**, *255*, 989–991.
- (a) Shalaby, F.; Rossant, J.; Yamaguchi, T. P.; Gertsenstein, M.; Wu, X.-F.; Breitman, M. L.; Schuh, A. C. Failure of blood-island formation and vasculogenesis in Flk-1-deficient mice. *Nature* **1995**, *376*, 62–66. (b) KDR is human receptor and Flk-1 is mouse receptor.
- Ferrara, N.; Gerber, H.-P.; LeCouter, J. The biology of VEGF and its receptors. *Nat. Med.* **2003**, *9*, 669–676.
- Kerbel, R. S. A cancer therapy resistant to resistance. *Nature (London)* **1997**, *390*, 335–336.
- Yang, J. C.; Haworth, L.; Sherry, R. M.; Hwu, P.; Schwartzentruber, D. J.; Topalian, S. L.; Steinberg, S. M.; Chen, H. X.; Rosenberg, S. A. A randomized trial of bevacizumab (anti-VEGF antibody) in metastatic renal cancer. *N. Eng. J. Med.* **2003**, *349*, 427–434.
- Prewett, M.; Huber, J.; Li, Y.; Santiago, A.; O'Connor, W.; King, K.; Overholser, J.; Hooper, A.; Pytowski, B.; Witte, L.; Bohlen, P.; Hicklin, D. J. Antivascular endothelial growth factor receptor (fetal liver kinase 1) monoclonal antibody inhibits tumor angiogenesis. *Cancer Res.* **1999**, *59*, 5209–5218.
- Holash, J.; Davis, S.; Papadopoulos, N.; Croll, S. D.; Ho, L.; Russell, M.; Boland, P.; Leidich, R.; Hylton, D.; Burova, E.; Ioffe, E.; Huang, T.; Radziejewski, C.; Baily, K.; Fandl, J. P.; Daly, T.; Wiegand, S. J.; Yancopoulos, G. D.; Rudge, J. S. VEGF-Trap: A VEGF blocker with potent antitumor effects. *Proc. Natl. Acad. Sci. U.S.A.* **2002**, *99*, 11393–11398.
- (a) Dreves, J.; Müller-Driver, R.; Wittig, C.; Fuxius, S.; Esser, N.; Huggenschmidt, H.; Konerding, M. A.; Allegrini, P. R.; Wood, J.; Hennig, J.; Unger, C.; Marmé, D. PTK787/ZK222584, a specific vascular endothelial growth factor-receptor tyrosine kinase inhibitor, effects the anatomy of the tumor vascular bed and the functional vascular properties as detected by dynamic enhanced magnetic resonance imaging. *Cancer Res.* **2002**, *62*, 4015–4022. (b) Bold, G.; Altman, K.-H.; Frei, J.; Lang, M.; Manley, P. W.; Traxler, P.; Wietfeld, B.; Brügger, J.; Buchdunger, E.; Cozens, R.; Ferrari, S.; Furet, P.; Hofmann, F.; Martiny-Baron, G.; Mestan, J.; Rösel, J.; Sills, M.; Stover, D.; Acemoglu, F.; Boss, E.; Emmenegger, R.; Lässer, L.; Masso, E.; Roth, R.; Schlachter, C.; Vetterli, W.; Wyss, D.; Wood, J. M. New anilinothalazines as potent and orally well absorbed inhibitors of the VEGF receptor tyrosine kinase useful as antagonists of tumor-driven angiogenesis. *J. Med. Chem.* **2000**, *43*, 2310–2323.
- (a) Mendel, D. B.; Laird, A. D.; Xin, X.; Louie, S. G.; Christensen, J. G.; Li, G.; Schreck, R. E.; Abrams, T. J.; Ngai, T. J.; Lee, L. B.; Murray, L. J.; Carver, J.; Chan, E.; Moss, K. G.; Haznedar, J. O.; Sukbunthorn, J.; Blake, R. A.; Sun, L.; Tang, C.; Miller, T.; Shirazian, S.; McMahon, G.; Cherrington, J. M. In vivo antitumor activity of SU11248, a novel tyrosine kinase inhibitor targeting vascular endothelial growth factor and platelet-derived growth factor receptors: Determination of a pharmacokinetic/pharmacodynamic relationship. *Clin. Cancer Res.* **2003**, *9*(1), 327–337. (b) Sepp-Lorenzino, L.; Thomas, K. A. *Expert Opin. Invest. Drugs* **2002**, *11*, 1–18.
- (a) Abdollahi, A.; Lipson, K. E.; Han, X.; Krempien, R.; Trinh, T.; Weber, K. J.; Hahnfeldt, P.; Hlatky, L.; Debus, J.; Howlett, A. R.; Huber, P. E. SU5416 and SU6668 attenuate the angiogenic effects of radiation-induced tumor cell growth factor production and amplify the direct anti-endothelial action of radiation in vitro. *Cancer Res.* **2003**, *63*(13), 3755–3763. (b) Sun, L.; Tran, N.; Liang, C.; Hubbard, S.; Tang, F.; Lipson, K.; Schreck, R.; Zhou, Y.; McMahon, G.; Tang, C. Identification of substituted 3-[(4,5,6,7-tetrahydro-1H-indol-2-yl)methylene]1,3-dihydroindol-2-ones as growth factor receptor inhibitors for VEGFR2 (Flk-1/KDR), FGF-R1, and PDGF-Rβ tyrosine kinases. *J. Med. Chem.* **2000**, *43*, 26655–26663.
- (a) Ciardiello, F.; Caputo, R.; Damiano, V.; Caputo, R.; Troiani, T.; Vitagliano, D.; Carlomagno, F.; Veneziani, B. M.; Fontanini, G.; Bianco, A. R.; Tortora, G. Antitumor effects of ZD6474, a small molecule vascular endothelial growth factor receptor tyrosine kinase inhibitor, with additional activity against epidermal growth factor receptor tyrosine kinase. *Clin. Cancer Res.* **2003**, *9*(4), 1546–1556. (b) Hennequin, L. F.; Stokes, E. S.; Thomas, A. P.; Johnstone, C.; Plé, P. A.; Ogilvie, D. J.; Dukes,

- M.; Wedge, S. R.; Kendrew, J.; Curwen, J. O. Novel 4-anilinoquinazolines with C-7 basic side chains: Design and structure activity relationship of a series of potent, orally active, VEGF receptor tyrosine kinase inhibitors. *J. Med. Chem.* **2002**, *45*, 1300–1312.
- (23) Kabbinnavar, F.; Hurwitz, H. I.; Fehrenbacher, L.; Meropol, N. J.; Novotny, W. F.; Lieberman, G.; Griffing, S.; Bergsland, E. Phase II, randomized trial comparing bevacizumab plus fluorouracil (FU)/leucovorin (LV) with FU/LV alone in patients with metastatic colorectal cancer. *J. Clin. Oncol.* **2003**, *21*(1), 60–65.
- (24) (a) Gingrich, D. E.; Reddy, D. R.; Iqbal, M. A.; Singh, J.; Almone, L. D.; Angeles, T. S.; Albom, M.; Yang, S.; Ator, M. A.; Meyer, S. L.; Robinson, C.; Ruggeri, B. A.; Dionne, C. A.; Vaught, J. L.; Mallamo, J. P.; Hudkins, R. L. A new class of potent vascular endothelial growth factor receptor tyrosine kinase inhibitors: Structure–activity relationships for a series of 9-alkoxymethyl-12-(3-hydroxypropyl)indeno[2,1-a]pyrrolo[3,4-c]carbazole-5-ones and the identification of CEP-5214 and its dimethylglycine ester prodrug clinical candidate CEP-7055. *J. Med. Chem.* **2003**, *46*, 5375–5388. (b) Boyer, S. J. Small molecule inhibitors of KDR (VEGFR-2) kinase: An overview of structure activity relationships. *Curr. Top. Med. Chem.* **2002**, *2*, 973–1000. (c) Connell, R. D. Patent focus on cancer chemotherapeutics V. Angiogenesis agents: September 2001–August 2002. *Expert Opin. Ther. Pat.* **2002**, *12*, 1763–1782.
- (25) Wolfe, J. P.; Buchwald, S. L. Palladium-catalyzed amination of aryl triflates. *J. Org. Chem.* **1997**, *62*, 1264–1267.
- (26) Reisch, J.; Dziemba, P.; Mura, M. L.; Rao, A. R. Natural product chemistry. part 159 [1]. Two methods for the synthesis of 4-azaacronycine as a potential antitumor agent. *J. Heterocycl. Chem.* **1993**, *30*, 981–983.
- (27) Brown, A. D.; Dickinson, R. P.; Wythes, M. J. Indole derivatives as 5-HT-like agonists WO 93/21178.
- (28) Farina, V.; Krishnan, B. Large rate accelerations in the Stille reaction with tri-2-furylphosphine and triphenylarsine as palladium ligands: Mechanistic and synthetic implications. *J. Am. Chem. Soc.* **1991**, *113*, 9585–9595.
- (29) Fujita, M.; Oka, H.; Ogura, K. Palladium(0)/LiCl promoted cross-coupling reaction of (4-pyridyl)stannanes and aromatic bromides: Easy access to poly(4-pyridyl)-substituted aromatics. *Tetrahedron Lett.* **1995**, *36*, 5247–5250.
- (30) Mann, G.; Hartwig, J. F.; Driver, M. S.; Fernández-Rivas, C. Palladium-catalyzed C–N(sp²) bond formation: N-Arylation of aromatic and unsaturated nitrogen and the reductive elimination chemistry of palladium azolyl and methyleneamido complexes. *J. Am. Chem. Soc.* **1998**, *120*, 827–828.
- (31) Sato, N.; Fujii, M. Studies on pyrazines. 29 [1]. High regioselective synthesis of choropyrazines from 3-substituted pyrazine 1-oxides. *J. Heterocycl. Chem.* **1994**, *31*, 1177–1180.
- (32) Lohse, O. Improved large-scale preparation of 4-iodopicolinic acid. *Synth. Commun.* **1996**, *26*, 2017–2025.
- (33) Kelly, T. R.; Kim, M. H. Synthesis of schumanniofytine and isoschumanniofytine. *J. Org. Chem.* **1992**, *57*, 1593–1597.
- (34) (a) Torrado, A.; Lopez, S.; Alvarez, R.; Lera, A. R. General synthesis of retionids and arotinoids via palladium-catalyzed cross-coupling of boronic acids with electrophiles. *Synthesis* **1995**, 285–293. (b) Torrado, A.; Imperiali, B. New synthetic amino acids for the design and synthesis of peptide-based metal ion sensors. *J. Org. Chem.* **1996**, *61*, 8940–8948.
- (35) Aoyagi, Y.; Inoue, A.; Koizumi, I.; Hashimoto, R.; Tokunaga, K.; Gohma, K.; Komatsu, J.; Sekine, K.; Miyafuji, A.; Kunoh, J.; Honma, R.; Akita, Y.; Ohta, A. Palladium-catalyzed cross-coupling reactions of chloropyrazines with aromatic heterocycles. *Heterocycles* **1992**, *33*, 257–272.
- (36) Vedejs, E.; Luchetta, L. M. A method for iodination of oxazoles at C-4 via 2-lithiooxazoles. *J. Org. Chem.* **1999**, *64*, 1011–1014.
- (37) Monaco, E. A., III; Vallano, M. L. Cyclin-dependent kinase inhibitors: Cancer killers to neuronal guardians. *Curr. Med. Chem.* **2003**, *10*, 367–379.
- (38) Senderowicz, A. M. Modulators of cyclin-dependent kinases: A novel therapeutic approach for the treatment of neoplastic diseases. *Cell Cycle Inhib. Cancer Ther.* **2003**, 179–205.
- (39) Fischer, P. M.; Gianella-Borradori, A. CDK inhibitors in clinical development for the treatment of cancer. *Exp. Opin. Invest. Drugs* **2003**, *12*, 955–970.
- (40) Grant, S.; Roberts, J. D. The use of cyclin-dependent kinase inhibitors alone or in combination with established cytotoxic drugs in cancer chemotherapy. *Drug Resistance Updates* **2003**, *6*(1), 15–26.
- (41) Kelland, L. R. Flavopiridol, the first cyclin-dependent kinase inhibitor to enter the clinic: Current status. *Exp. Opin. Invest. Drugs* **2000**, *9*, 2903–2922.
- (42) Grosios, K. UCN-01 Kyowa Hakko Kogyo Co. *Curr. Opin. Invest. Drugs* **2001**, *2*, 287–297.
- (43) (a) Ruetz, S.; Fabbro, D.; Zimmermann, J.; Meyer, T.; Gray, N. Chemical and biological profile of dual Cdk1 and Cdk2 inhibitors. *Curr. Med. Chem.: Anti-Cancer Agents* **2003**, *3*(1), 1–14. (b) Zimmermann, J. Pharmacologically active pyridine derivatives and processes for the preparation thereof. *PCT Int. Pat.* 1995, WO 9509853.
- (44) (a) Thornber, C. W. Isosterism and molecular modification in drug design. *Chem. Soc. Rev.* **1979**, *8*, 563–580. (b) Horwell, D. C.; Nichols, P. D.; Roberts, E. Methionine replacements in biologically active peptides. *Bioorg. Med. Chem. Lett.* **1994**, *4*, 2263–2266.
- (45) Brogi, E.; Wu, T.; Namiki, A.; Isner, J. M. Indirect angiogenic cytokines upregulate VEGF and bFGF gene expression in vascular smooth muscle cells, whereas hypoxia upregulates VEGF expression only. *Circulation* **1994**, *90*, 649–652.
- (46) Kilic, T.; Alberta, J. A.; Zdunek, P. R.; Acar, M.; Iannarelli, P.; O'Reilly, T.; Buchdunger, E.; Black, P. M.; Stiles, C. D. Intracranial inhibition of platelet-derived growth factor-mediated glioblastoma cell growth by an orally active kinase inhibitor of the 2-phenylaminopyrimidine class. *Cancer Res.* **2000**, *60*, 5143–5150.
- (47) The 17-fold higher potency of compound **15** exhibited in VEGF-stimulated HUVEC proliferation (IC₅₀ = 0.005 μM) as compared to the VEGFR-2 kinase inhibition (IC₅₀ = 0.084 μM) suggests that **15** may inhibit another part of the VEGFR-2 signaling pathway in the stimulated HUVEC cells other than VEGFR-2 inhibition, such as ERK1, FGFR1, Tie2, VEGFR-1.
- (48) Furet, P.; Zimmermann, J.; Capraro, H.-G.; Meyer, T.; Imbach, P. Structure-based design of potent CDK1 inhibitors derived from olomoucine. *J. Comput.-Aided Mol. Des.* **2000**, *14*, 403–409.
- (49) Emanuel, S.; Gruninger, R. H.; Fuentes-Pesquera, A.; Connolly, P. J.; Seamon, J. A.; Hazel, S.; Tominovich, R.; Hollister, B.; Napier, C.; Reuman, M.; Bignan, G.; Tuman, R.; Johnson, D.; Moffatt, D.; Batchelor, M.; Foley, A.; O'Connell, J.; Allen, R.; Perry, M.; Jolliffe, L.; Middleton, S. A. A VEGF-R2 kinase inhibitor potentiates the activity of the conventional chemotherapeutic agents paclitaxel and doxorubicin in tumor xenograft models. *Mol. Pharm.* **2004**, *66*, 635–647.
- (50) McTigue, M. A.; Wickersham, J. A.; Pinko, C.; Showalter, R. E.; Parast, C. V.; Tempczyk-Russell, A.; Gehring, M. R.; Mroczkowski, B.; Kan, C.-C.; Villafranca, J. E.; Appel, K. Crystal structure of the kinase domain of human vascular endothelial growth factor receptor 2: A key enzyme in angiogenesis. *Structure* **1999**, *7*, 319–330.
- (51) Maestro, Schrodinger, 1500 S. W. First Avenue, Suite 1180, Portland, OR 97201.
- (52) Still, W. C.; Tempczyk, A.; Hawley, R. C.; Hendrickson, T. Semianalytical treatment of solvation for molecular mechanics and dynamics. *J. Am. Chem. Soc.* **1990**, *112*, 6127–6129.
- (53) Gray, N. S.; Wodicka, L.; Thunnissen, A.-M. W. H.; Norman, T. C.; Kwon, S.; Espinoza, F. H.; Morgan, D. O.; Barnes, G.; LeClerc, S.; Meijer, L.; Kim, S.-H.; Lockhart, D. J.; Schultz, P. G. Exploiting chemical libraries, structure, and genomics in the search for kinase inhibitors. *Science* **1998**, *281*, 533–538.
- (54) Prime, Schrodinger, 1500 S. W. First Avenue, Suite 1180, Portland, OR 97201.
- (55) Glide, Schrodinger, 1500 S. W. First Avenue, Suite 1180, Portland, OR 97201.
- (56) Friesner, R. A.; Banks, J. L.; Murphy, R. B.; Halgren, T. A.; Klicic, J. J.; Mainz, D. T.; Repasky, M. P.; Knoll, E. H.; Shelley, M.; Perry, J. K.; Shaw, D. E.; Francis, P.; Shenkin, P. S. Glide: A new approach for rapid, accurate docking and scoring. 1. Method and assessment of docking accuracy. *J. Med. Chem.* **2004**, *47*, 1739–1749.
- (57) MacroModel, Schrodinger, 1500 S. W. First Avenue, Suite 1180, Portland, OR 97201.
- (58) Jorgensen, W. L.; Maxwell, D. S.; Tirado-Rives, J. Development and testing of the OPLS all-atom force field on conformational energetics and properties of organic liquids. *J. Am. Chem. Soc.* **1996**, *118*, 11225–11235.

JM040099A